Smart Operation of Centralized Temperature Control System in Multi-Unit Residential Buildings

by

Rajib Kundu

A thesis
presented to the University of Waterloo
in fulfillment of the
thesis requirement for the degree of
Master of Applied Science
in
Electrical and Computer Engineering

Waterloo, Ontario, Canada, 2013

I hereby declare that I am the sole author of this thesis. This is a true copy of the thesis, including any required final revisions, as accepted by my examiners.

I understand that my thesis may be made electronically available to the public.

Abstract

Smart Grid has emerged a very important concept in modern power systems. The integration of different loads such as residential, commercial and industrial into the smart grid and their optimal operation has a significant effect on the system's reliability, stability, peak power demand and energy price.

This work presents the mathematical modeling of a Centralized Temperature Control System (CTCS) of a Multi-Unit Residential Building (MURB) and its optimal operation considering electricity prices and weather variations. The model considers comfort levels, preference settings and activity of residents in different units of the building to determine the optimal operation schedules of the CTCS, minimizing its total energy consumption cost. Multi-objective operation of the MURB is also investigated when residents in different units have conflicting interests, and the impact of such conflicting preferences on the operation of CTCS is analyzed. A case-study on optimal energy management of a single unit house considering net-metering is also presented.

The proposed CTCS model is a Mixed Integer Non Linear Programing (MINLP) model, where some of the constraints are linearized to reduce the computational complexity arising from the non-linearity, for real-time applications. The model is studied for various customers' preferences using a realistic MURB model. Simulation results show that significant cost savings can be achieved using the proposed mathematical model.

Acknowledgments

I would first like to thank God who gave me the health, strength and patience to complete this job. I would like also to express my sincere gratitude to my supervisors Professor Kankar Bhattacharya and Professor Claudio A. Cañizares, for their excellent guidance and complete support.

This work was funded by NSERC Smart Microgrid Network (NSMG-Net). Funding received from the project to carry out this research is gratefully acknowledged.

I would like to thank Dr. Steve Wong, CanmetENERGY for his insightful comments and suggestion, at various stages of the work.

I would like to extend my thanks to Professor Ian Rowlands and Professor Stephen L. Smith for serving as my thesis readers and providing valuable feedback on my research work. Their constructive comments and valuable suggestions are greatly appreciated.

I am grateful to my former lab mate, Dr. Sumit Paudyal, for his help, support, and encouragement, and the NSMG-Net project team members, Felipe Ramos Gaete and Rupali Jain for their cooperation and support. Special thanks to Trevor Kanerva, Chief Operating Engineer from Plant Operations Department at the University of Waterloo for his help to model the cooling and heating system. Finally, I would like to thank my uncle Rajendra Nath Kundu, PEng., without whose consistent support, my pursuit of graduate studies would remain an untouched dream.

Dedication

This Work is Dedicated to My Beloved Mother.

Table of Contents

List of Tables **ix**

List of Figures **x**

Nomenclature **xii**

1 Introduction **1**

1.1 Motivation 1

1.2 Literature Review 3

1.2.1 Smart Grid and Residential Energy Management Systems 3

1.2.2 Centralized Temperature Control Systems 6

1.3 Research Objectives 8

1.4 Thesis Organization 9

2 Background **10**

2.1 Residential EMS Model 10

2.1.1 Mathematical Model 11

2.1.2 Case Studies 14

2.1.3 Simulation Results and Analysis 18
2.2 Temperature Control Systems in Residential Units 27
2.2.1 Centralized Temperature Control Systems (CTCS) 27
2.2.2 Decentralized Temperature Control Systems 29
2.3 Summary 30

3 Smart Operational Framework of MURB **31**
3.1 Proposed Supervisory Temperature Control System 31
3.2 Mathematical Modeling of the Proposed System 32
3.2.1 Objective Functions 33
3.2.2 Model Constraints 34
3.2.3 Linearization of Constraints 38
3.3 Summary 39

4 Case Studies **40**
4.1 MURB Example 40
4.2 Model Inputs 41
4.3 Results and Analysis 43
4.3.1 TOU Pricing 44
4.3.2 RTP Scheme 46
4.3.3 Multi-Objective Optimization 49
4.4 Computational Aspects 52
4.5 Summary 53

5 Conclusions and Future Work **54**

5.1 Summary and Conclusions 54

5.2 Contributions 55

5.3 Future Work 55

Bibliography **56**

List of Tables

2.1 Comparison of Energy Cost and Savings of Devices with Different Pricing Schemes 25

4.1 Temperature limits for MURB units 42

4.2 Comparison of electrical energy consumption and cost 48

4.3 Comparison of savings in total energy consumption and cost 49

List of Figures

1.1 Sector-wise energy demand of Canada [2]. 1

1.2 Source-wise energy generation mix in Ontario for 2011 [4]. 2

1.3 Sector-wise energy consumption in Canada for 2011 [1]. 2

1.4 Breakdown of total energy usage in a residential house [8]. 4

1.5 Conceptual model of the Smart Grid. 5

2.1 Two-meter model. 11

2.2 Net-meter model. 11

2.3 Four different price signals for a summer day (Jul 21, 2011) in Toronto [31]. 16

2.4 Outside temperature of a summer day (Jul 21, 2011) in Toronto [32]. . . . 16

2.5 Solar power generation profile for a 3 kW solar PV panel in Toronto [33]. . 16

2.6 Hot-water consumption pattern for a typical day [21]. 17

2.7 Typical activity level of the household [21]. 17

2.8 Base load demand profile assumed. 17

2.9 Optimal operational schedule of AC and variation of indoor temperature with different energy prices for Case 1. 19

2.10 Optimal operational schedule of water heater with different energy prices for Case 1. 20

2.11 Optimal operational schedule of battery charging, discharging and storage level of battery with different energy prices for Case 1. 21
2.12 Optimal operational schedule of AC and variation of indoor temperature with different energy prices for Case 2. 22
2.13 Optimal operational schedule of water heater with different energy prices for Case 2. 23
2.14 Optimal operational schedule of battery charging and discharging and storage level with different energy prices for Case 2. 24
2.15 Total energy cost for different cases with different energy prices. 25
2.16 Centralized temperature control system (CTCS). 28

3.1 Hierarchical structure of supervisory and existing CTCS. 32

4.1 Geometric characteristics of an MURB. 40
4.2 Electricity pricing schemes of a summer weekday in Toronto (Jul 22, 2011) [31]. 42
4.3 Activity level for all units. 43
4.4 Temperature of a warm summer day in Toronto (Jul 22, 2011). 43
4.5 Indoor temperature variation of Zone 1 for different Cases, with TOU. . . . 45
4.6 Optimal schedule of central AC for different Cases, with TOU. 46
4.7 Indoor temperature variation of Zone 1 for different cases, with HOEP. . . 47
4.8 Optimal schedule of central AC for different cases, with HOEP. 48
4.9 Variation of J_M with the variation of multi-objective function weights. . . . 50
4.10 Variation of total cost with the variation of multi-objective function weights. 50
4.11 Variation of J_1 and J_2 with the variation of multi-objective function weights. 51
4.12 Variation of total energy consumption with the variation of multi-objective function weights. 52

Nomenclature

Indices

i	Devices; $i = \{$Central AC (ac), Heater (ht),fan (f),cooling valve (cv), heating valve (hv), air mixing unit $(m)\}$
t	Time intervals
z	Zones

Sets

A	Set of devices; $A = \{ac, ht, f, cv, hv, m\}$
T	Set of indices for simulation time limit

Variables

$S_i(z,t)$	State of device i of zone z at time t; continuous and discrete (ON/OFF)
$\theta_p(t)$	Water temperature in primary water-loop at time t [° C]
$\theta_z(t)$	Inside temperature of zone z at time t [° C]
$q_f(z,t)$	Effect of circulated air-flow of zone z at time t
$P_D(t)$	Power demand of single unit house at time t [kW]
$ESL_{pv}(t)$	Energy storage level in battery at time t [kWh]
$\theta_{wh}(t)$	Water temperature in the water heater [° C]
$\theta_in(t)$	Inside temperature of single unit house at time t [° C]
$I_1(z,t)$	Multidimensional binary variables
$I_2(z,t)$	Multidimensional binary variables
$FM(z,t)$	Multidimensional binary variables

Parameters

τ	Simulation step interval duration [0.25 hr]
P_i	Rated power of a device [kW]
Q_{ht}	Gas to heat conversion rate of central heater [Btu/kWh]
$C_{ed}(t)$	Electricity pricing rate [$/kWh]
C_{FIT}	Feed-In-Tariff rate [0.8 $/kWh]
$P_G(t)$	Power generated from solar panel at time t [kW]
$\theta_{out}(t)$	Forecasted outside temperature [°C]
γ_{ac}	Cooling capacity of central AC [kJ/hr]
κ_{ht}	Heating capacity of central heater [kJ/hr]
m	Max^m water flow rate in primary water loop [kg/hr]
m_z	Max^m water flow rate in heat exchanging coil [kg/hr]
S	Specific heat of water [4200 J/(kg K)]
γ_z	Cooling capacity of a zonal valve when it is fully open [kJ/hr]
κ_z	Heating capacity of a zonal valve when it is fully open [kJ/hr]
C_z	Total heat capacity of a zone [kJ/K]
$AL_z(t)$	Activity level in zone z at time t [p.u.]
$\beta_{act}(t)$	Heat generation co-efficient due to activity level [kJ/(hr K)]
α_z	Thermal leakage of zone z [kJ/(hr K)]
$\alpha_w h$	Water heater heat co-efficient [kJ/(hr K)]
β_z	Cooling effect of supply fan [kJ/(hr K)]
$\beta_w h$	Water heater thermal loss co-efficient [°C/interval]
$\gamma_w h$	Cooling effect on hot water temperature due to activity level [°C/p.u.]
$HWU(t)$	Hot water usage at time t [Ltr]
U	Heat transfer co-efficient of building's wall [1.33 W/(m^{2}K)]
A_z	Area of zone z [m^2]
ρ_a	Density of air [1.27 kg/m^3]
C_a	Specific heat of air [1.006 kJ/(kg K)]
$ESL_{pv}^{min}(t)$	Minimum energy storage level in battery at time t [kWh]

$ESL_{pv}^{max}(t)$	Maximum energy storage level in battery at time t [kWh]
$Q_a^{leak}(z)$	Air leakage of zone z [m^3/hr]
$Q_a^{max}(z)$	Maximum^{m}air flow rate of supply fan in zone z [m^3/hr]
$\theta_z^l(t)$	Lower limit of inside temperature of zone z at time t [°C]
$\theta_z^u(t)$	Upper limit of inside temperature of zone z at time t [°C]
$\theta_{wh}^{min}(t)$	Lower limit of water temperature in water heater at time t [°C]
$\theta_{wh}^{max}(t)$	Upper limit of water temperature in water heater at time t [°C]
C_1	Auxiliary constant; to scale down temperatures [100 p.u.]
C_2	Minimum opening of air mixture when the fan is ON [0.1 p.u.]
C_3	Auxiliary constant [0.9999 p.u.]
UB	Upper band temperature [7°C]
LB	Lower band temperature [35°C]
η_{ac}	Efficiency of central AC [p.u.]
η_{ht}	Efficiency of central heater [p.u.]
J	Objective functions

Chapter 1

Introduction

1.1 Motivation

The total energy demand of Canada is comparatively higher than that of the other countries, because of its geographical location and high living standards. The total energy demand of Canada was approximately 2978 TWh in 2011 [1], and the end-use demand is envisioned to grow at 1.3% annually over the next 23 years [2]. Figure 1.1 presents

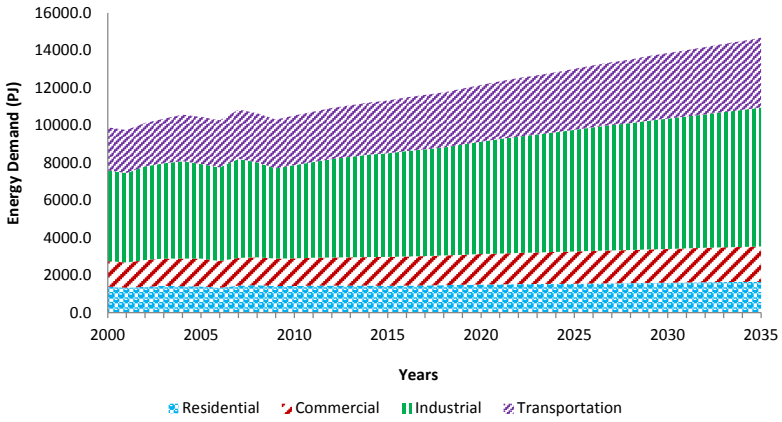

Figure 1.1: Sector-wise energy demand of Canada [2].

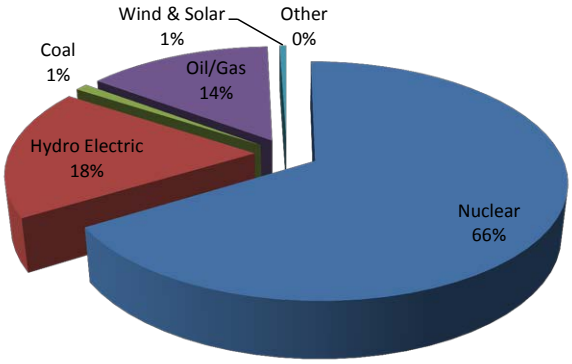

Figure 1.2: Source-wise energy generation mix in Ontario for 2011 [4].

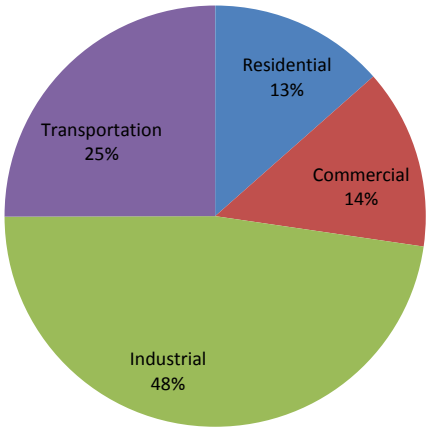

Figure 1.3: Sector-wise energy consumption in Canada for 2011 [1].

the sector-wise energy demand forecast for Canada over a 35 year period. Also, the government of Ontario has planned to shut down all its coal fired plants by 2014 to reduce carbon emissions [3]. This reduction in generation capacity needs be compensated by clean sources of energy, which will change the energy generation mix in the coming years. The generation mix for 2011 is illustrated in Figure 1.2.

Figure 1.3 presents the sector-wise energy consumption in Canada for 2011. The residential sector's energy demand growth rate is expected to be 0.6% per year. Statistics Canada indicates that approximately 36% of the Canadian population lives in multi-unit

apartment buildings, and these account for about 24% of the annual energy consumption of the residential sector [5]-[6]. Hence, energy savings in this customer segment would have a significant impact on total energy consumption.

Canadian households use energy to heat or cool their home spaces, light their homes, heat water, and to run various electrical appliances such as stoves, refrigerators, televisions and computers. On an average, a household in Ontario consumes 106 GJ of energy each year [7]. Space heating and cooling account for the major share of the residential energy consumption, as illustrated in Figure 1.4. It is also reported in [8] that almost 50% of the monthly household electricity cost is from space heating and/or cooling.

In order to save energy, researchers worldwide have are examining new energy saving approaches for space heating and cooling appliances to reduce energy costs. With the advent of Smart Grids and other associated technologies, energy management of HVAC and other household electrical appliances can be accomplished in real-time, in a robust and convenient manner. Thus, this thesis proposes and discusses the mathematical modeling of a Centralized Temperature Control System (CTCS) of a Multi-Unit Residential Building (MURB) and its optimal operation considering electricity prices and weather variations.

1.2 Literature Review

1.2.1 Smart Grid and Residential Energy Management Systems

The Smart Grid refers to an automated, widely distributed energy delivery network, characterized by a two-way flow of electricity and information, with monitoring capabilities of power plants, customer preferences, and individual appliances. These grids will incorporate distributed computing and communications to deliver real-time information and enable the near-instantaneous balance of supply and demand, at the device level [9]. These advanced intelligent communication technology and superior control systems will enable the grid to link consumers and utility control center in real-time. Thus, energy usage optimization in different load sectors is becoming an important issue in Smart Grids [10]-[11].

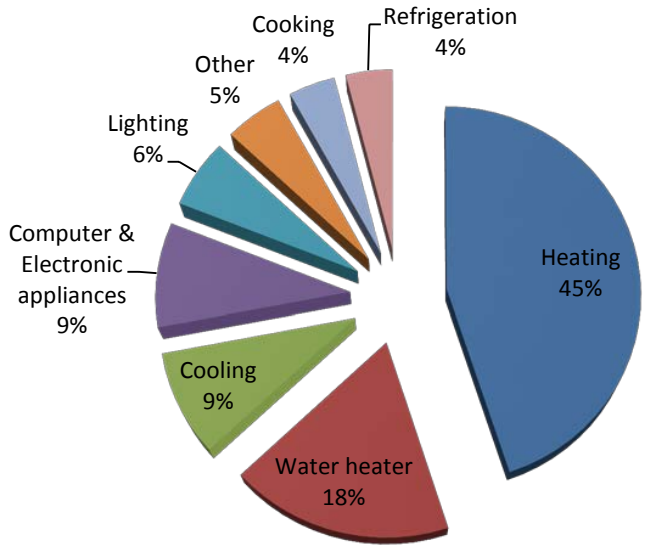

Figure 1.4: Breakdown of total energy usage in a residential house [8].

To meet the growing energy demand, various load management techniques have been adopted and proposed. Although Direct Load Control (DLC) has existed for decades to control residential loads, Demand Response (DR) techniques have become one of the most promising resources in the context of Smart Grids, due to their ability to intelligently meet the requirements of end-user loads [12]. According to the Federal Energy Regulatory Commission (FERC), DR is defined as the changes in electric usage by end-use customers from their normal consumption patterns in response to changes in price of electricity over time, or incentive payments designed to induce lower electricity use at times of high wholesale market prices or when system reliability is jeopardized [13]. DR programs can either be incentive-based (e.g., direct load control) or time-based (e.g., dynamic pricing, critical peak pricing), depending on the purpose of the utility [14]. Typically, DR is incentive based, with end-users reducing their consumption during peak demand periods when receiving incentives. A full automated Energy Management System (EMS) is necessary for time-based DR programs, so that load can be automatically shifted according to time varying pricing schemes [15].

The main benefits of EMS, specially for end-users, are the effective management of

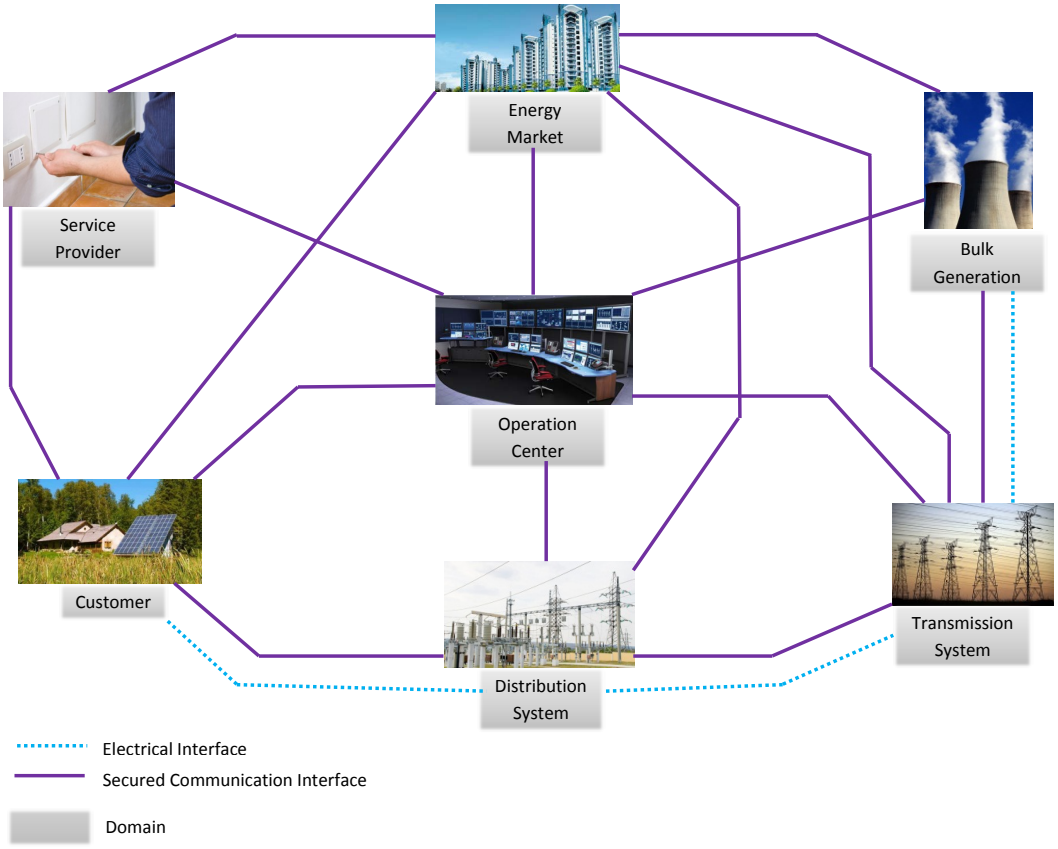

Figure 1.5: Conceptual model of the Smart Grid.

energy requirements, intelligent control of major electrical loads, and application of automatic and instantaneous DR technology to maximize energy savings. However, the successful implementation of EMS requires the Advanced Metering Infrastructure (AMI), which comprises smart metering, local area networks, and integrated communication systems [16]. These provide a two-way communication link between customers and utility service providers to manage and control energy consumption [17]. Smart metering allows the customers to monitor different loads, as well as enabling them to communicate with the utility in a secure manner. A conceptual description of modern smart grid is illustrated in Figure 1.5.

DSM (Demand Side Management) and DR programs have been envisioned as tools

for unlocking the full potential of the smart grid, and achieving energy and cost savings through proper use of EMS [18]. The application of DSM techniques on pilot projects has been reported in [19]. The primary target in this case is to reduce the peak demand only, and the task is performed by using one-way Very High frequency (VHF) radio to send ON/OFF signals for some pre-selected devices at the customers' premises. The Electric Power Research Institute (EPRI) was the first to introduce in 1980 DR in power grids. In 1981, the Omaha Public Power District launched demand limit control experiment among fifty customers; a penalty provision worth \$0.50/occurrence for customers overriding the utility's control signal was enforced. In 1984, the Florida Power Corporation and Florida Power and Light Company (FPL) implemented similar projects using VHF and two-way power line communication for DLC and peak load shaving; FPL reported an achievement of 1000 MW peak load savings. Similar projects were also implemented in South Korea, Japan, England, and France in the '90s, all aiming at peak shaving.

In the late '90s, Ontario Hydro launched DLC programs for residential customers' electric water heater. Approximately 16% of the 1.6 million residential customers participated in this program, and the total number of electric water heaters were 260,000. Most of these water heaters were controlled and centrally dispatched, while some had individual timer controllers. The main control strategy was to turn OFF the water heater during peak demand periods. Individual water heater load reductions were in the range of 0.5-0.8 kW, for a total of 45-67 MW of demand reduction. Incentives were offered to customers for participating in this program [20].

1.2.2 Centralized Temperature Control Systems

In the residential sector, Multi-unit Residential Buildings (MURB) could achieve significant cost savings through smart energy management of the Heating, Ventilation and Air-conditioning (HVAC) system. In most cases, a MURB has a centralized temperature control system for all units.

Various methods have been proposed in the literature to model the MURB's Centralized Temperature Control System (CTCS) for controlling the temperature of each unit

simultaneously. The mathematical modeling of temperature control systems and other energy elements such as lighting, various electrical appliances (water heater, dish washer, refrigerator, washer, dryer, stove, solar PV, and batteries) of a single residential house is described in the context of Smart Grids in [21]. A hygrothermal model for HVAC system and multi-zone building model is proposed in [22], which simulates combined heat, vapor and liquid transfer in porous elements and the HVAC system; however, the computational burden makes it unsuitable for integration in real-time supervisory control systems. Optimization of energy consumption based on electricity and natural gas price is proposed in [23], which includes thermal and electrical storage options.

A smart sensor web network model is proposed as an EMS in [24], to minimize the energy consumption of the centralized AC of a residential building based on the ambient room temperature setting. Simulation results show that application of the EMS can significantly reduce the energy consumption of AC. In [25], a multi-objective heating optimization model with a combined approach of traditional ξ-constraint and goal programming methods is proposed. This model solves the problem of space heating of a single house under a time-varying electricity price while minimizing three objectives: heating energy cost, heating energy consumption, and deviation of temperature from the resident's defined temperature setting.

The impact of DR in residential buildings on the operation of an electric power distribution system is investigated in [26]. A modified IEEE-13 bus system, including over a thousand single-unit residential loads, is used with a combination of ZIP and physical load models. Each unit's HVAC system is controlled through an active controller on the basis of dynamic energy pricing. Though the customers' preferences are considered, the external weather conditions are not included in the model; moreover, a detailed model of the HVAC system and building characteristics is needed for the exact control of household temperature. A novel residential EMS with different levels of automation for implementing DR in a single unit house is proposed in [27]. The model neglects the activity level in the house which may have significant impact on the room temperature. Moreover, the integration of the model for real-time control appears to be a very cumbersome job, as the modeling of different appliances are conducted at various platforms.

In [28],a simplified model of a district heating/cooling system of a MURB complex is developed, and its accuracy in quantifying the heating or cooling demand of a large building is validated through a series of simulations. Energy supply and distribution in the system is optimized considering the heating/cooling demand, which is estimated using their historical data. This approach can lead to excessive heating or cooling in some units, since it provides heating or cooling to all units simultaneously and uniformly. A multi-agent control framework is proposed in [29] to find an optimal solution between energy consumption cost and users comfort levels for a smart building complex. A multi-objective particle swarm optimization and a weighted aggregation based optimization approach are proposed to generate Pareto fronts which are made up of Pareto-optimal solutions. Moreover, multi-layer controller agents for each user are modeled to control decentralized HVAC, illumination, and carbon dioxide concentration in a centralized way.

1.3 Research Objectives

Most of the work discussed in the literature review section are focused on the detailed physical modeling of a single unit centralized or decentralized temperature control systems. No work has been reported in the literature, so far, focusing particularly on the reduction of the electrical energy cost of a MURB through real-time, smart operation of its CTCS, and integrating the model into an EMS. Thus, in the present work, a comprehensive mathematical model of a MURB is developed for real-time, smart operation of CTCS. This model considers residents' activity level, weather and energy forecast data to schedule the operation of CTCS in a cost-effective way. Hence, the main objectives of this research work are as follows:

- Develop a mathematical optimization model of the MURB, including the CTCS operational constraints, representing the indoor temperature dynamics of the MURB, which is to be maintained within the customers' preferred levels.
- Validate the effectiveness of the proposed model based on a realistic MURB example.

- Test the proposed model's capability to handle multiple conflicting preferences of different customers through a multi-objective optimization approach.

1.4 Thesis Organization

This thesis is divided into five chapters. Chapter 2 presents relevant background such as the EMS model of a single-unit residential house, the description of different MURB temperature control systems, and the proposed smart operational framework of the CTCS of a MURB. Chapter 3 outlines the conceptual framework of the proposed supervisory control system; the mathematical model of the CTCS and the estimation of the required model parameters are also discussed in this chapter. In Chapter 4, a MURB example and the inputs to the model are presented, and the results of several case-studies are discussed. Finally, in Chapter 5, a summary and the main conclusions and contributions of the present work are presented; the scope for future work is also discussed.

Chapter 2

Background

2.1 Residential EMS Model

A residential customer in the context of Smart Grids can have various electrical appliances, energy storage systems (such as batteries, electric vehicles), small-scale energy production systems (such as Photo Voltaic (PV) solar panels and wind power), and a smart metering system which enables two-way communication link between these components. The residential EMS refers to the coordinated and optimal use of these components considering electricity prices, aimed at reducing the system peak demand, household energy consumption level cost, and/or maximizing renewable energy utilization etc. This task can be accomplished by the smart metering infrastructure and two-way communication such as the home area network.

In Smart Grids, residential customers can use and sell the electrical energy generated from small-scaled generation systems installed in their premises while buying energy from the grid. A case study is undertaken here on a single-unit residential house to study this problem, based on a previously proposed EMS model that forms the basis to the models proposed in this thesis. This EMS model enables customers to buy and sell energy to the grid in real-time. The mathematical model, constraints, model inputs, and relevant results pertaining to this study are described next.

2.1.1 Mathematical Model

The basic mathematical model of a single-unit house used in this work is adopted from [21], and is described next. The energy consumption of the house is simulated for three cases: base case (Case 0), two-meter model (Case 1), and net-meter model (Case 2). The two-meter model and net-meter model are depicted in Figures 2.1 and 2.2, respectively.

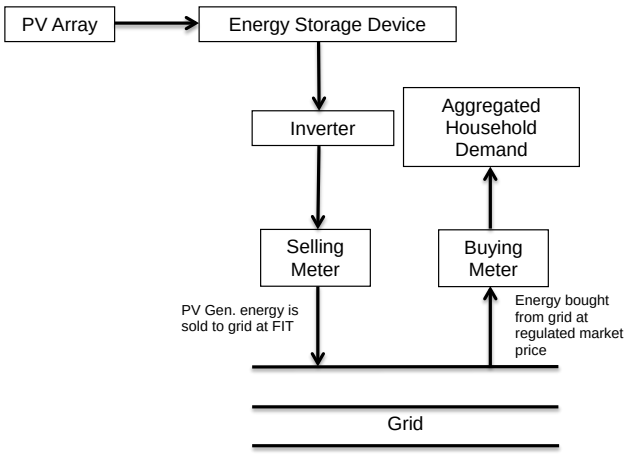

Figure 2.1: Two-meter model.

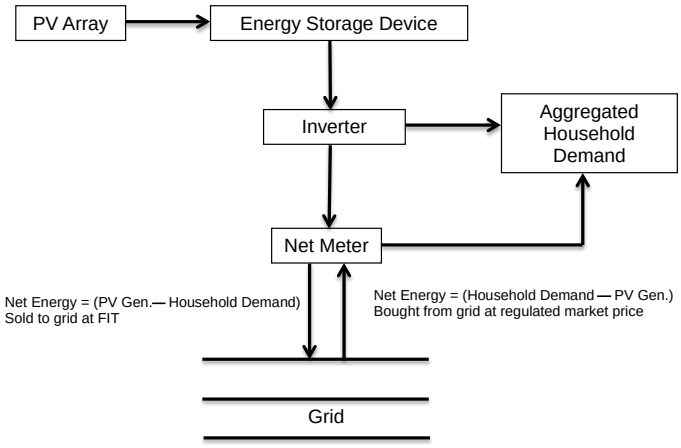

Figure 2.2: Net-meter model.

Objective Functions

- Case-0: Maximizing resident's comfort level by minimizing temperature deviation from customer's preferred settings.

$$J_1 = \sum_{t \in T} |\theta_z(t) - \theta^{set}| \tag{2.1}$$

All variables, functions, and parameters in this and other equation are defined in the Nomenclature Section.

- Case-1: Minimization of total electrical energy cost of the household considering the two-meter model. In this case, one meter is used to buy energy from the grid, and other is used to sell all generated energy from solar PV panels at a FIT rate.

$$J_2 = \sum_{i \in (ht,wh)} \sum_{t \in T} \tau C_D(t) P_i S_i(t) - \sum_{i \in (pv)} \sum_{t \in T} \tau C_{FIT} P_G(t) \tag{2.2}$$

- Case-2: Minimization of total electrical energy cost of the household considering the net-meter model. In this case, energy buying and selling is done through a single smart meter; thus, only the energy remaining after meeting the household demands is sold to the grid.

$$J_3 = \begin{cases} C_D(t)(P_D(t) - P_G(t)) & \text{if } P_D(t) \geq P_G(t) \\ C_{FIT}(P_G(t) - P_D(t)) & \text{if } P_D(t) < P_G(t) \end{cases} \quad \forall t \in T \tag{2.3}$$

Model Constraints

In the proposed model, the following three electrical appliances are modeled in detail, while the rest of the electrical appliances of the household are considered as an aggregated base load whose consumption varies with the activity level of the residents.

- **PV Solar Array**

The considered PV solar array is equipped with energy storage system. Thus, the modeling of battery charging and discharging is incorporated in the proposed model as follows:

$$chd_{pv}(t) = \begin{cases} P_{chd} & \text{if } P_{pv}(t) \geq P_{chd} \\ P_{pv} & \text{if } P_{pv} \leq P_{chd} \end{cases} \quad \forall t \in T \tag{2.4a}$$

$$ESL_{pv}(t) = ESL_{pv}(t-1) + \tau[S_{pv}^{chd}(t)chd_{pv}(t) + S_{pv}^{dch}(t)dch_{pv}(t)] \quad \forall t \in T \tag{2.4b}$$

$$ESL_{pv}^{min}(t) \leq ESL_{pv}(t) \leq ESL_{pv}^{max}(t) \qquad \forall t \in T \tag{2.4c}$$

$$S_{pv}^{chd}(t) + S_{pv}^{dch}(t) \leq 1 \qquad \forall t \in T \tag{2.4d}$$

Constant battery charging operation is simulated by (2.4a). For simplicity, it is assumed that the battery voltage remains constant during charging and discharging, simulating its operation with (2.4b). Equation (2.4d) ensures that the converter could not operate in charging and discharging mode simultaneously. It is assumed that the conversion efficiency is 100%.

- **Water Heater**

Inter-temporal dependency and average consumption of hot water per day in the household, and the thermodynamical characteristics of the water heater at time t are modeled as follows:

$$\theta_{wh}(t) = \theta_{wh}(t-1) + \tau\left[\alpha_{wh}S_{wh}(t) - \beta_{wh}HWU(t) - \gamma_{wh}\right] \qquad \forall t \in T \tag{2.5a}$$

$$\theta_{wh}^{min}(t) \leq \theta_{wh}(t) \leq \theta_{wh}^{max}(t) \tag{2.5b}$$

Upper and lower temperature limit of hot water are represented by (2.5b).

- **Temperature Control System**

  In addition to the maximum temperature deviation that the resident is willing to tolerate, the temperature control system model also includes: ambient temperature; heat loss or gain through walls; and the heat generated by the residents' activities.

$$\theta_{in}(t) = \theta_{in}(t-1) + \tau \Big[\beta_{act} AL(t) + \kappa_{ht} S_{ht}(t) - \gamma_{ac} S_{ac}(t) + \alpha_z(t)(\theta_{out} - \theta_{in}) \Big] \qquad \forall t \in T \tag{2.6a}$$

$$S_{ac}(t) + S_{ht}(t) \leq 1 \tag{2.6b}$$

$$\theta^{min}(t) \leq \theta(t) \leq \theta^{max}(t) \tag{2.6c}$$

Equation (2.6b) guarantees that the AC and heater cannot be in operation simultaneously, and the residents preferred temperature limits are represented by (2.6c).

2.1.2 Case Studies

A single-unit house in Ontario equipped with a 3.0 kW solar panel and an associated 30 kWh battery are considered in this work. Each case defined earlier is simulated for four different energy pricing schemes: Time of Use (TOU), Real time pricing (RTP), Fixed Rate Price (FRP) and Locational Marginal Pricing (LMP), as illustrated in Figure 2.3. Outdoor temperature data, solar power generation profile, hot water consumption data, and activity level of the household are incorporated in the model as input parameters. All the case studies are conducted for a warm summer day (July 21, 2011) to quantify the savings. The input parameters are defined as follows:

- The Hourly Ontario Energy Price (HOEP) and Ontario TOU schemes are adopted as RTP and TOU in this work, respectively. Note that the HOEP does not correspond in practice to the actual consumer price, since further adjustments are viable to this value; hence, this is used in this thesis as a proxy for RTP, without loss of generality, in view of the lack of public information with respect to actual prices. The greater

Toronto Area's GTAA-LT.G_M12 nodal energy price is taken as LMP, without further adjustment and loss of generality, while the FRP is 0.9 $/kWh, which is taken from [21], considering the household energy consumption to be above the threshold level of 600 kWh/month. For all these pricing schemes, historical data has been used in the present simulations; however, it is assumed that all these price information would be available to customers through energy price forecast tool, on a day-ahead basis.

- The outdoor temperature profile of the summer day considered is given in Figure 2.4.
- An approximated solar PV power generation profile (Figure 2.5), depending on the solar radiation of the considered day, is obtained using the following equation [30]:

$$P_G(t) = 3000[1+\{25-\theta_{out}(t)\}]\times(-0.0034)\times(ShortwaveSolarRadiation(Wm^2)/1000) \tag{2.7}$$

  The simulated solar power profile is depicted in Figure 2.5.
- The hot water consumption and activity level of the house are illustrated in Figures 2.6 and 2.7, respectively.
- An base load consumption pattern depending on a typical household energy consumption data and activity level is assumed, as illustrated in Figure 2.8.
- The FIT is considered as 0.8 $/kWh in this work.

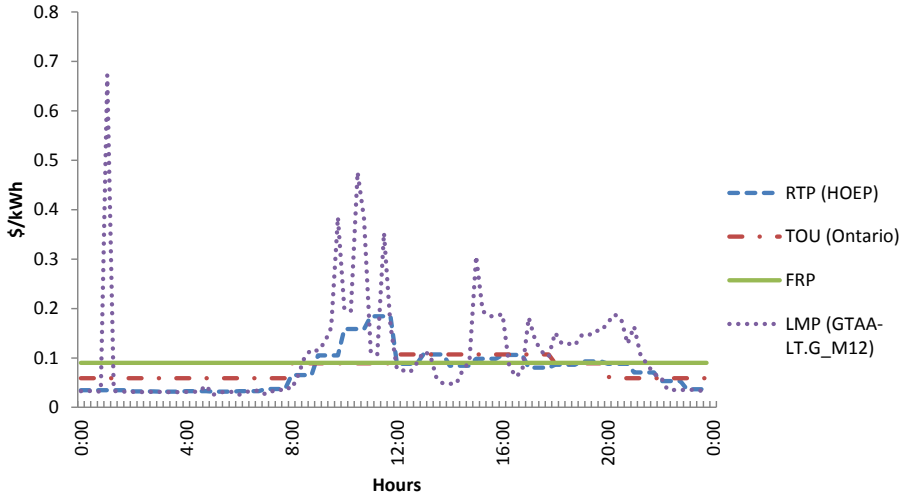

Figure 2.3: Four different price signals for a summer day (Jul 21, 2011) in Toronto [31].

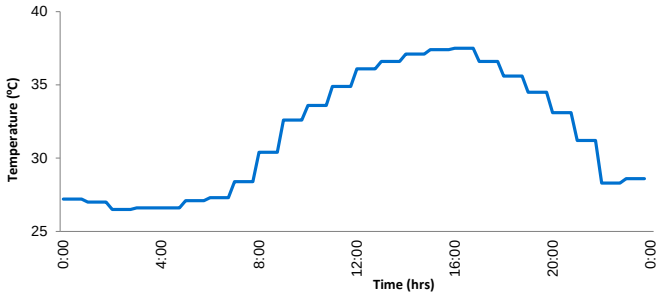

Figure 2.4: Outside temperature of a summer day (Jul 21, 2011) in Toronto [32].

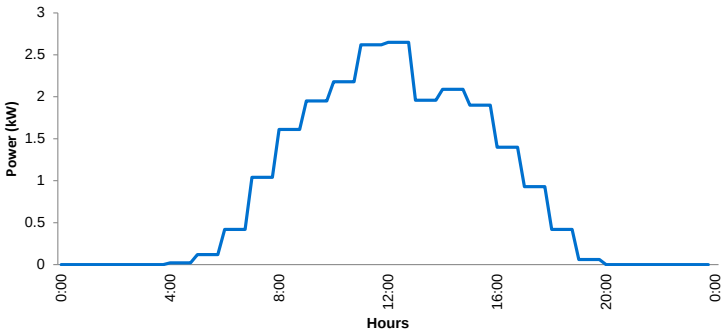

Figure 2.5: Solar power generation profile for a 3 kW solar PV panel in Toronto [33].

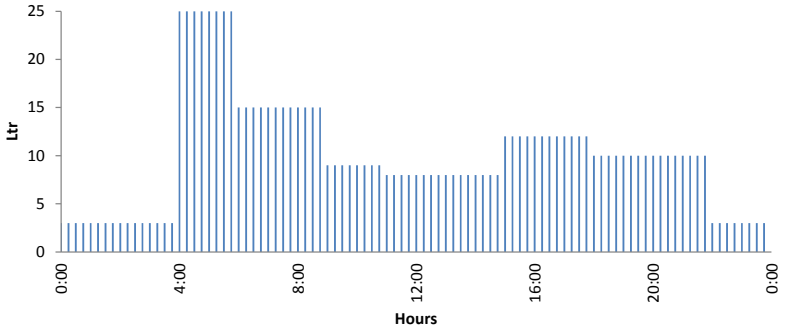

Figure 2.6: Hot-water consumption pattern for a typical day [21].

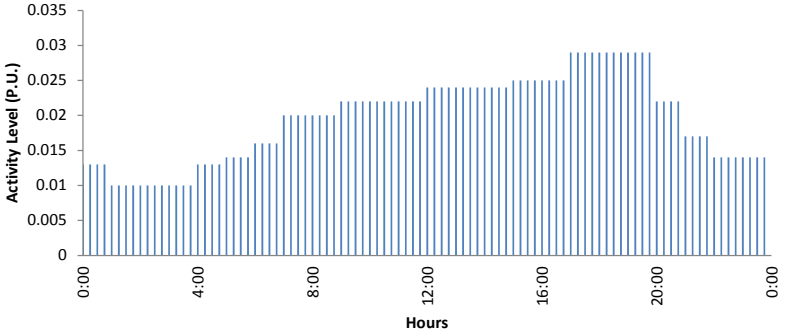

Figure 2.7: Typical activity level of the household [21].

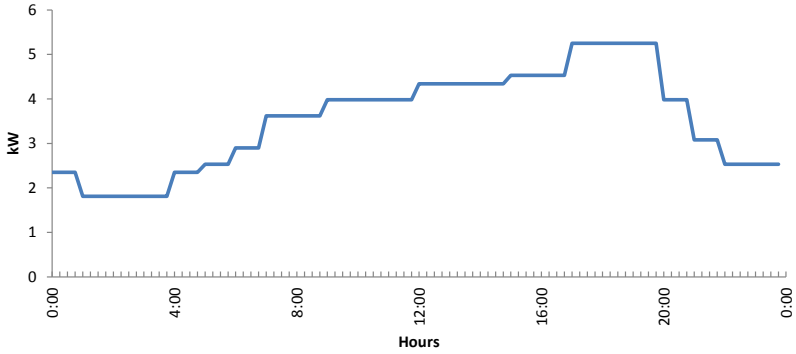

Figure 2.8: Base load demand profile assumed.

2.1.3 Simulation Results and Analysis

The obtained results are summarized next to quantify the prospective energy savings that could be achieved by deploying the proposed model for a single-unit residential house. The optimal operational schedules of PV solar array, water heater, and AC are determined for the three cases using the four pricing schemes (RTP, TOU, FRP, and LMP) discussed earlier.

Figures 2.9, 2.10, and 2.11 illustrate, for Case 1, the optimal operational schedules of AC, water heater and PV battery, respectively. As the main objective function of Case 1 is to minimize the electrical energy cost, the proposed optimization model seeks to reduce the number of turning ON events of the AC and water heater. It also seeks to maximize the number of discharging states of the battery to sell the generated energy to the grid at the FIT rate. Note that, in this case, it is assumed that the residential customer can sell all the PV generated energy to the grid.

From Figure 2.9 it is noted that, the optimization model seeks to turn ON the AC during the low price period, unless it is necessary to maintain the temperature within the customer's defined limits. For the FRP scheme, on the other hand, the AC is turned ON from 12.45 PM to maintain the temperature within the constraint envelope.

Since, the same hot water consumption pattern is considered for all pricing schemes, the optimal operational schedules of water heater remain almost identical. Small variations are observed in scheduling because of the variation of low price periods in different pricing schemes, as illustrated in Figure 2.10.

The PV array starts to charge its battery as soon as sunlight becomes available. Thus, until 4 AM, there is no charging and the battery cannot discharge because the energy level is at its minimum. When the energy level of the battery is higher than the specified minimum, it starts to discharge to reduce the energy consumption cost. Around 1 PM the battery's energy level reaches its maximum capacity limit; hence, it starts discharging despite sunlight being available. Through the charging and discharging events, the optimization model seeks to keep the battery's energy level as high as possible until sunset.

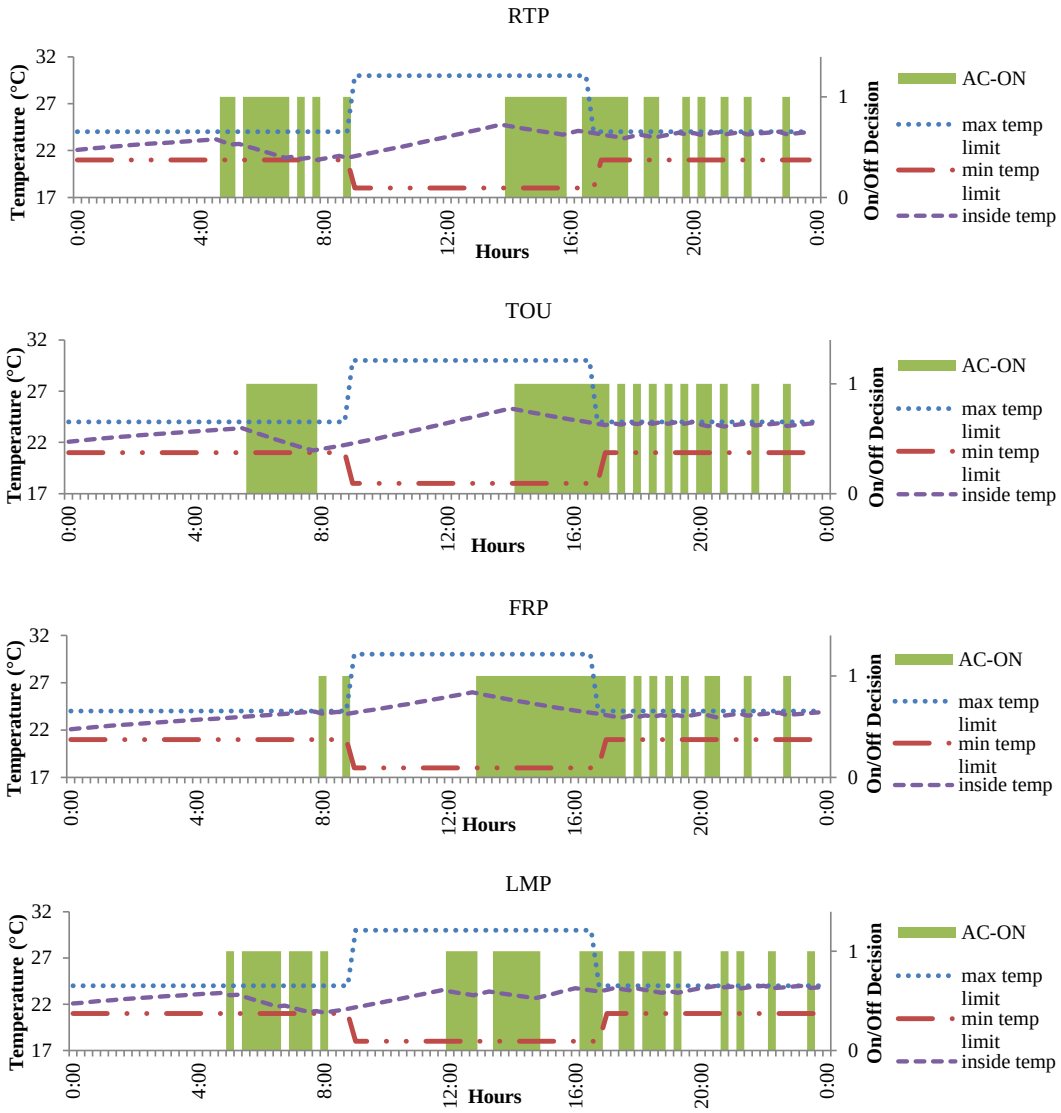

Figure 2.9: Optimal operational schedule of AC and variation of indoor temperature with different energy prices for Case 1.

Around 8 PM, when sunlight is no longer available, it starts to discharge, and continues discharging until the energy level reaches its specified minimum energy level.

Case 2 corresponds to the net-metering model where generated PV energy is sold to

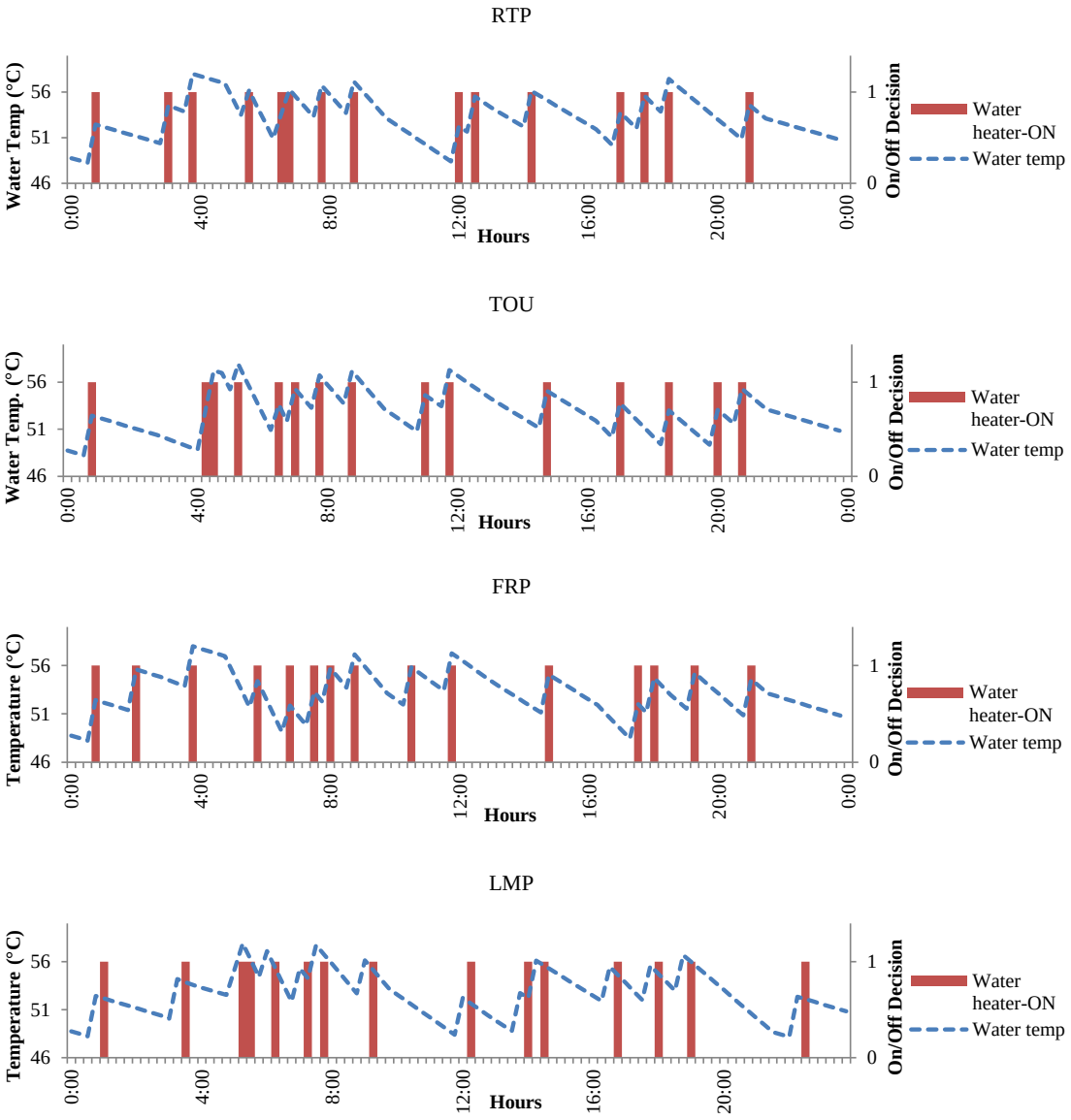

Figure 2.10: Optimal operational schedule of water heater with different energy prices for Case 1.

the grid at any instant after meeting the household demand. Thus the operation schedules of AC and water heater remain almost the same as in Case 1, as illustrated in Figures 2.12 and 2.13. Small variations in the schedules of AC and water heater are observed,

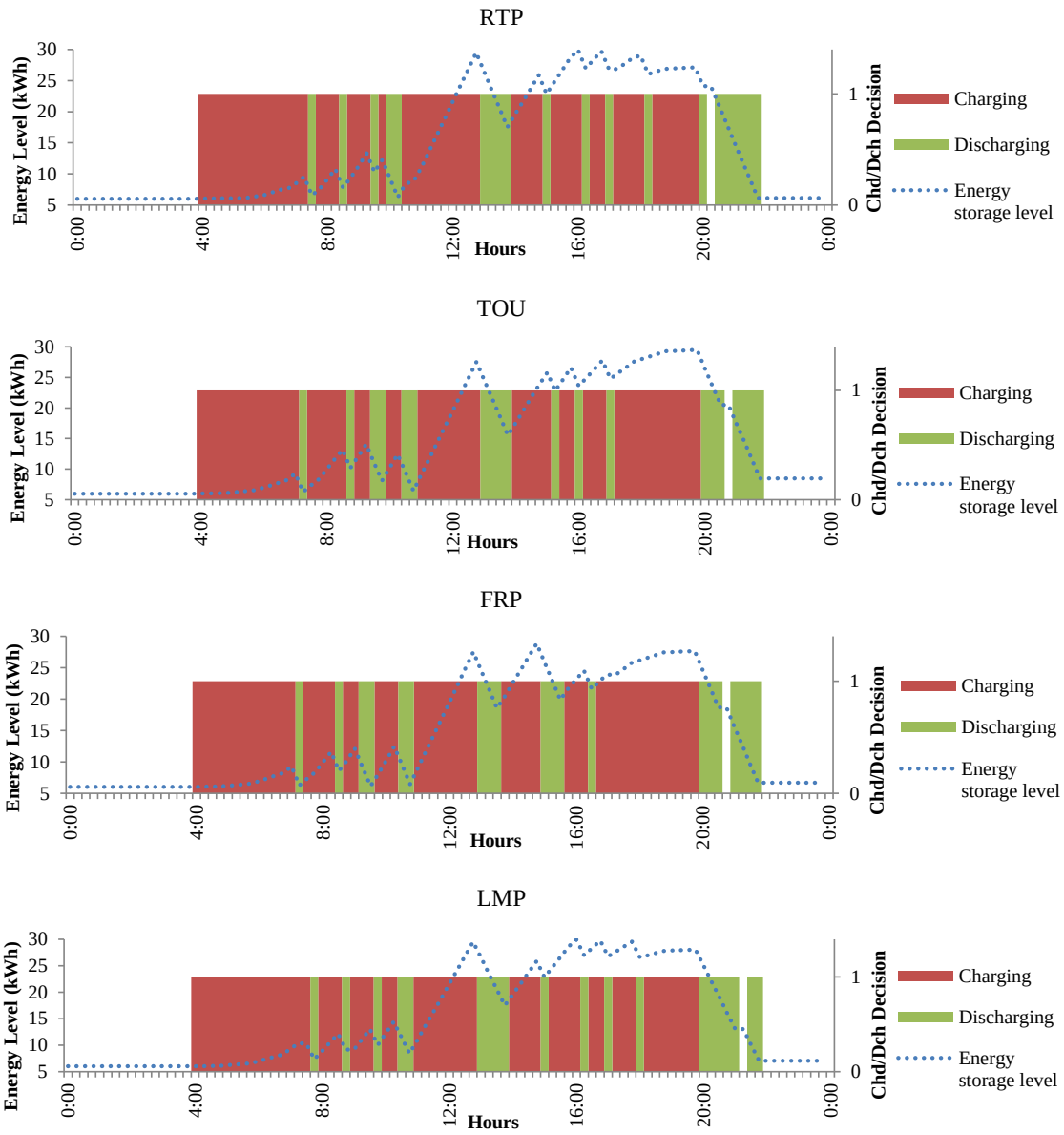

Figure 2.11: Optimal operational schedule of battery charging, discharging and storage level of battery with different energy prices for Case 1.

which can be attributed to the fact that the solver finds separate locally optimal solutions for different pricing schemes. However, the operation schedules of the PV battery are

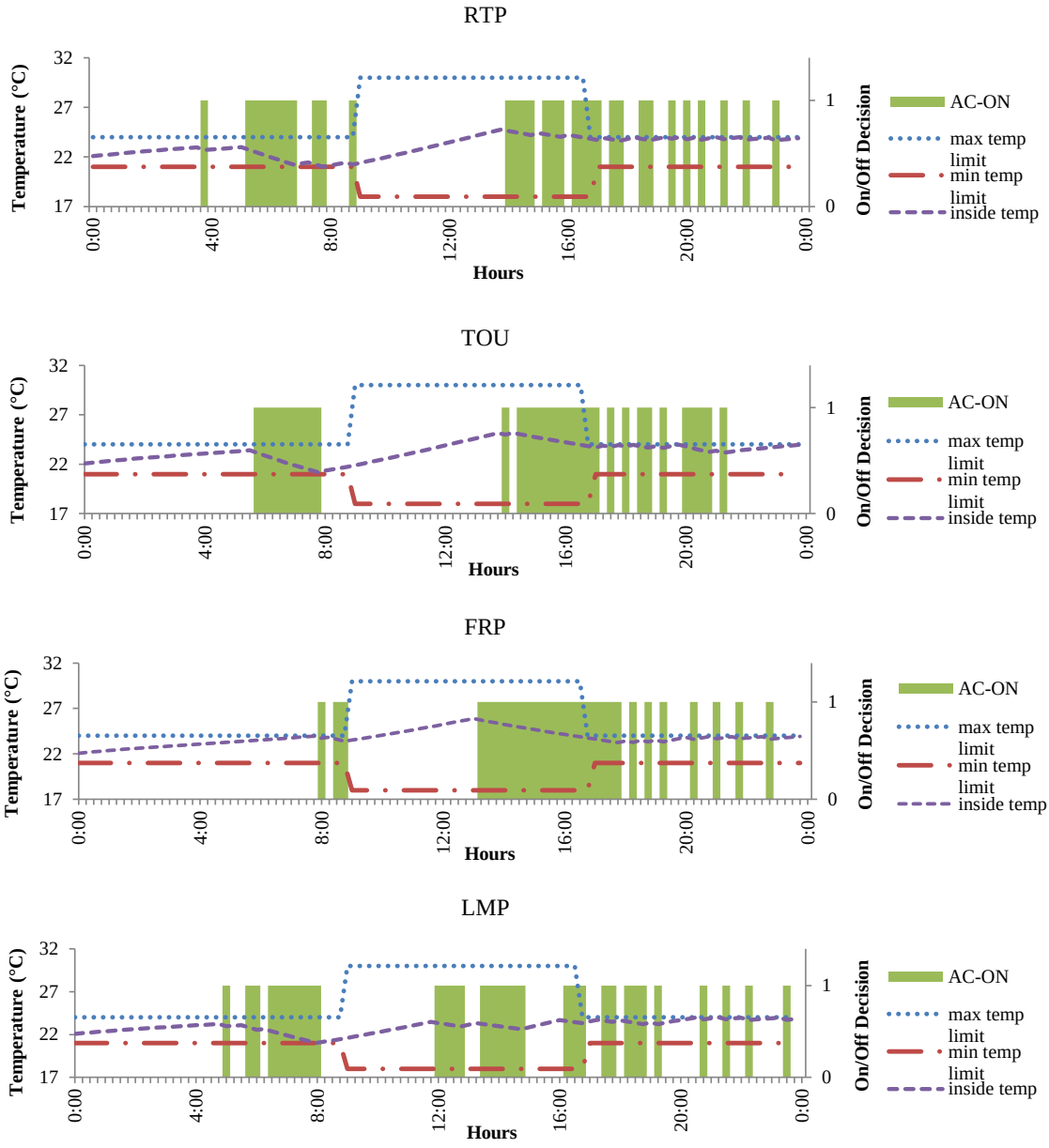

Figure 2.12: Optimal operational schedule of AC and variation of indoor temperature with different energy prices for Case 2.

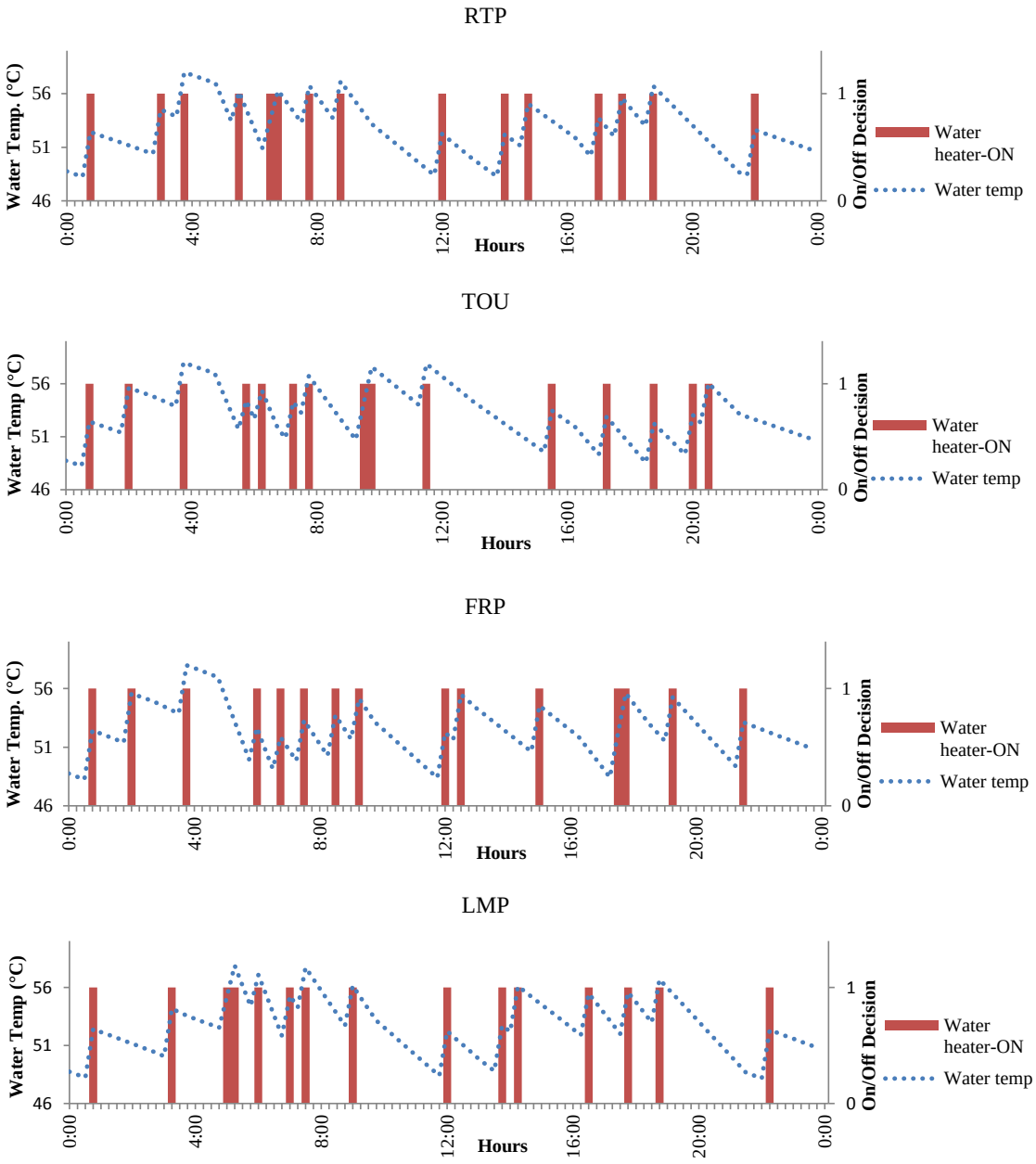

Figure 2.13: Optimal operational schedule of water heater with different energy prices for Case 2.

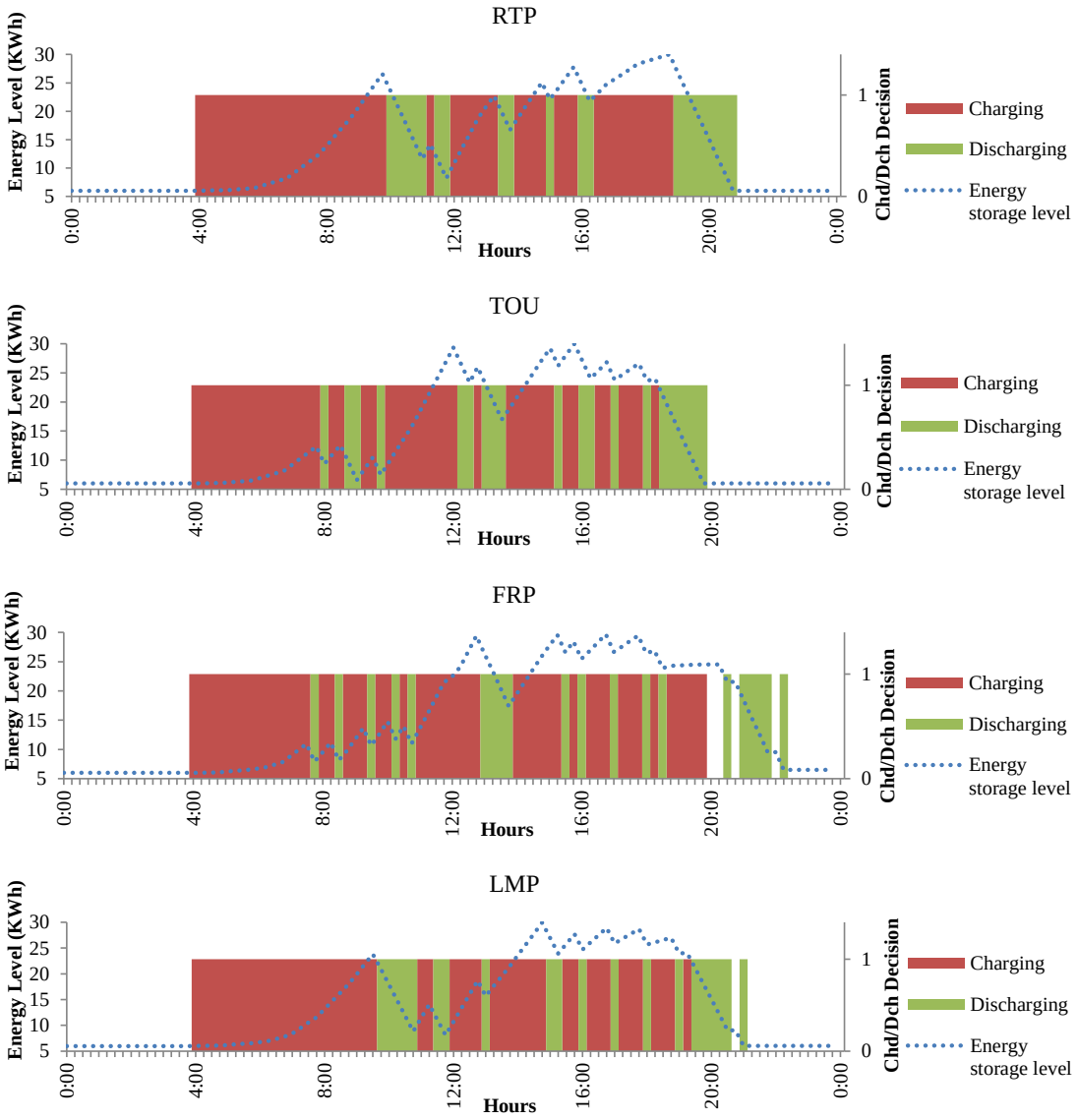

Figure 2.14: Optimal operational schedule of battery charging and discharging and storage level with different energy prices for Case 2.

significantly different than Case 1 for different pricing schemes, as shown in Figure 2.14, . In Case 2, the battery charging takes place during the off peak periods as much as possible, and discharges during the peak periods. However, in this case, the discharge period varies

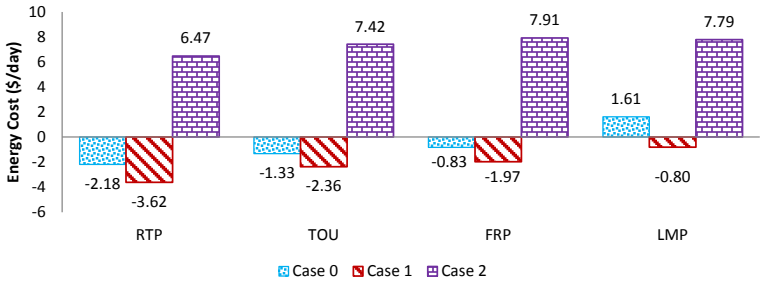

Figure 2.15: Total energy cost for different cases with different energy prices.

along the pricing schemes because of the variation in peak periods.

A comparative study of customer energy cost considering the four pricing schemes are illustrated in Figure 2.15. Observe that the lowest total cost is always obtained in Case 1 for all pricing schemes, because the optimization model seeks to maximize the sell of PV generated energy to the grid at FIT price. In Case 0, the RTP, TOU and FRP pricing schemes result in a negative cost to the customer, which indicates profit, because of the long sunny summer day, and the PV generated energy selling revenue being higher than the cost of consumed energy from the gird. In Case 2, all pricing schemes end up with a positive cost, as PV generated energy is sold to the grid only after meeting the household demand.

Table 2.1: Comparison of Energy Cost and Savings of Devices with Different Pricing Schemes

	Air Conditioner			Water Heater		
Pricing Schemes	Case 0 ($/day)	Case 1 ($/day)	Savings w.r.t to case 0 (%)	Case 0 ($/day)	Case 1 ($/day)	Savings w.r.t to case 0 (%)
LMP	3.089	1.241	59.832	0.204	0.122	39.920
RTP	2.266	1.207	46.719	0.165	0.131	20.090
TOU	2.818	2.104	25.332	0.183	0.171	6.240
FRP	2.970	2.129	28.333	0.213	0.203	4.706

From Table 2.1, the highest savings in the electrical energy cost is obtained for LMP, followed by RTP, FRP, and TOU. Device-wise energy cost is comparatively higher for TOU and FRP than for LMP and RTP, because of the more dynamic and lower pricing structure of LMP and RTP. Significant cost savings are obtained for the AC

The main conclusions of this study can be summarized as follows:

- In terms of aggregated energy costs, the lowest cost is obtained with RTP during summer.
- As compared to the base case, there is significant reduction in energy cost in Case 1 for all price signals.
- The energy cost for individual devices is reduced considerably, with the AC having the most significant reduction in its electrical energy cost for LMP and RTP.
- The schedules for charging and discharging of the battery change slightly for different pricing signals, because of multiple local solutions. However, the total number of charging and discharging events, and hence revenue from solar PV, remains the same.
- The schedules are not affected by solar PV for the net-meter case (Case 2).
- The study confirms that using two meters instead of net metering is beneficial from the customer's point of view, as expected.

2.2 Temperature Control Systems in Residential Units

Residential houses can be of several types, such as single units, multi-unit single floor, or multi-unit high rise apartments. Demand of heating or cooling of a building varies according to its size, structure, orientation and geographical location. There are several types of temperature control system available in the market. Each of them can satisfy HVAC objectives with different degrees of success. Temperature control system can be broadly classified into two main categories: Centralized and Decentralized systems. However, several kind of systems are available within each category depending on the different types of buildings.

2.2.1 Centralized Temperature Control Systems (CTCS)

CTCS serve multiple spaces from one base location. These type of units typically use chilled water as a cooling medium and use extensive ductwork for air distribution. Cooling (chilled water) is generated in a chiller at one base location and distributed to air-handling units or fan-coil units located throughout the building spaces. The air is cooled with secondary media (chilled water) and is transferred through air distribution ducts.

The system is broken down into three major subsystems: the chilled water plant, the condenser water system (or heat rejection system), and the air-delivery system. However, a central heater could be added to the system depending upon the geographical location. In that case, ductwork gets doubled. With the advancement of control mechanism, various new energy efficient control features have been developed such as constant air volume system, variable air volume system, air mixing unit, humidifier/ dehumidifier, etc. Any combination of these units can be used for the maximum efficiency of the system depending on the purpose and need of the building [34].

The main advantages of CTCS are better control of comfort conditions, higher energy efficiency, and greater load-management potential. The main drawbacks of these systems are that these more expensive to install and usually more sophisticated to operate and maintain.

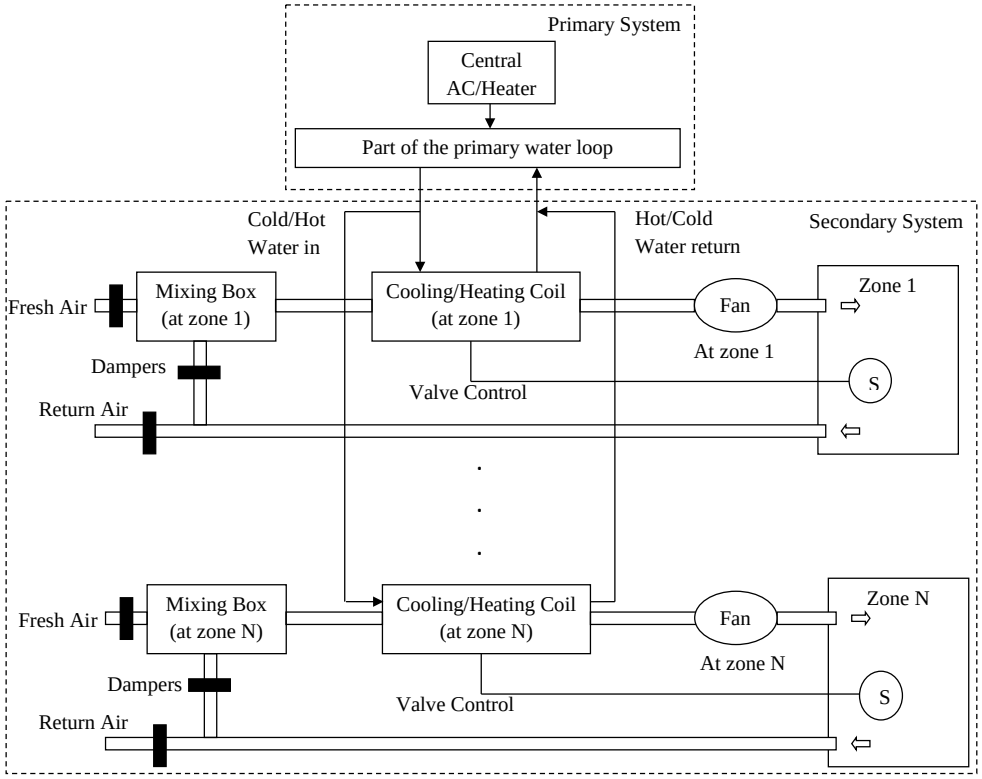

Figure 2.16: Centralized temperature control system (CTCS).

The CTCS used in this work is divided into two sub-systems, as illustrated in Figure 2.16. The first part is the primary system which comprises one air-cooled water chiller, one natural gas fired heater, a primary water circulation loop, and two water circulation pumps. The chiller and the heater come into operation according to the seasonal demand and cannot be in operation simultaneously. In the summer, the chiller comes in operation and maintains the main loop water temperature between 5°C and 7°C, and the water pumps keep the water circulating through the primary water loop. Each zone has its own secondary system which is connected to the primary system through a cooling/heating coil. The secondary system comprises three components: mixing box, cooling/heating coil, and supply fan. In case of intra-zoning, one unit could have several zones according to need, comfort level, and the building's geographical location. The heat exchanging coils

are responsible for cooling or heating of the incoming air from the mixing box, which mixes the indoor air partially with incoming fresh air, maintaining ASHRAE standards [35], and then circulates it in the respective zones; frequently, on-off based control systems are used for all zones. The programmable thermostat S determines the zone temperature at every interval and acts on the valve opening, if necessary. The effect of partial recirculation of inside air is modeled in this work in a simplified manner, so that this energy saving strategy can be represented in the proposed control approach.

2.2.2 Decentralized Temperature Control Systems

A decentralized temperature control system usually serve a single or small space from a location within or directly adjacent to that space. These are essentially direct expansion type and include:

- Packaged through-the-wall and window air conditioners.
- Interconnected room by room systems.
- Residential and light commercial split systems.
- Self-contained (floor by floor) systems.
- Commercial outdoor packaged systems.

The principal advantages of decentralized temperature control systems are lower initial costs, simplified installation, no heavy ductwork, independent zone control, and less floor space requirements for mechanical room, ducts, and pipes. Moreover, decentralized systems can be metered individually at each unit very easily. The disadvantages of these systems are short equipment life (less than 10 years), higher noise, higher energy consumption (kW/ton), and that's why these are not adequate where precise environmental conditions are required [34].

2.3 Summary

This chapter discuses several relevant background issues regarding the operation and implementation of EMS in residential units. An EMS in which the present work is based, was described, and a case study was carried out on a single-unit house, focusing on net-metering applications in the residential sector, and the effects of four different pricing schemes on household's electrical energy consumption cost. Different types of temperature control systems available in the market were also briefly discussed, concentrating on the CTCS used in this work.

Chapter 3

Smart Operational Framework of MURB

3.1 Proposed Supervisory Temperature Control System

A hierarchical control strategy for the MURB CTCS discussed in Chapter 2, is proposed here, as illustrated in Figure 3.1. The proposed optimization engine has two main parts: One is the supervisory control system where the developed mathematical model is integrated and external data are given as input signals. The other part is the existing control system in which decision signals are processed and deployed, turning ON/OFF devices according to these signals. Feedback from the existing controller goes to the new supervisory controller to ensure smooth operation of the proposed temperature control system. If there are any large incongruities between measured and calculated parameters, the feedback is used to run the optimization model again and determine new operational set points for each device based on a Model Predictive Control approach.

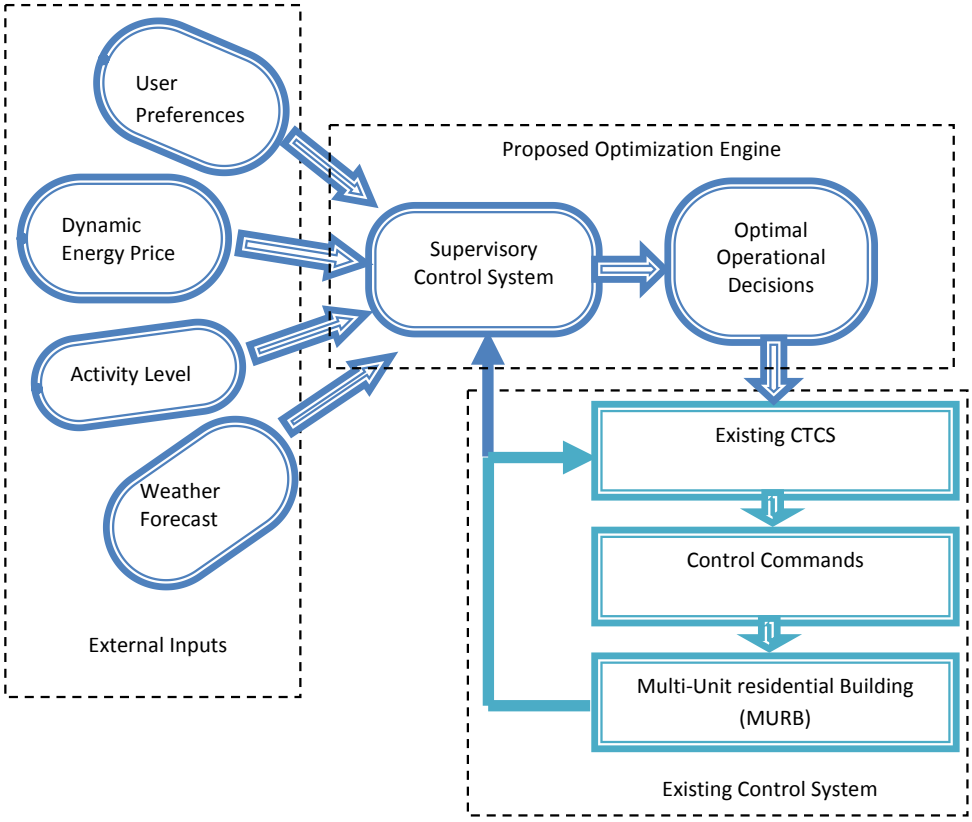

Figure 3.1: Hierarchical structure of supervisory and existing CTCS.

3.2 Mathematical Modeling of the Proposed System

The CTCS of MURBs can be of different types depending on the building's structure and its geographical location. The proposed CTCS considers a centralized heating and cooling device, primary water circulation loop, air mixing units and one supply fan for each zone, as discussed in Chapter 2. The mathematical models of these components and the proposed optimization approach are described next.

3.2.1 Objective Functions

Minimization of Temperature Deviations

This objective function seeks to track the user defined temperature closely by minimizing the sum of the absolute value of temperature deviation from the given set point, at each interval, as follows:

$$J_1 = \sum_z \sum_{t \in T} |\theta_z(t) - \theta_z^{set}| \tag{3.1}$$

This objective is used to represent the existing operation strategy of CTCS for comparison purposes.

Minimization of Total Energy Cost

The total energy consumption cost of the MURB over the scheduling horizon is minimized using the following objective function:

$$J_2 = \sum_z \sum_{t \in T} \sum_{i \in A} \tau \, C_{ed}(t) \, P_i(z) \, S_i(z,t) \tag{3.2}$$

It is assumed that residents in different units have the same objective, but they can have different preferred temperature settings.

Minimization of Total Energy Consumption

The total energy consumption of the system over scheduling horizon is minimized using the following objective function:

$$J_3 = \sum_z \sum_{t \in T} \sum_{i \in A} \tau \, P_i(z) \, S_i(z,t) \tag{3.3}$$

Multi-objective Optimization

When customers in different units have different priorities, i.e., different objective functions, the composite objective function of the CTCS can be represented using individual customer preferences, with associated weights, as follows:

$$J_M = \mu \frac{J_1}{J_1^*} + \psi \frac{J_2}{J_2^*} + \sigma \frac{J_3}{J_3^*} \tag{3.4}$$

where J_1^*, J_2^* and J_3^* are the optimal values of J_1, J_2 and J_3 when these functions are optimized individually. The associated weights μ, ψ and σ denote the relative importance of each objective function, and can vary from 0 to 1.

3.2.2 Model Constraints

Outside temperature, activity of the occupants, heat loss through walls, heat leakage through insulation, and heat transfer amongst the zones affect the inside temperature of a MURB. Thus, the proposed model should be able to represent the effect of these conditions, keeping the MURB unit temperatures within their pre-defined ranges while considering the characteristics of the CTCS. The operational constraints representing these phenomena and the control system are explained next.

Primary System Modeling

The primary system model includes the central heating and cooling unit, main water loop, and the effect of each valve opening on the temperature of the main water loop. The heat balance equation between the primary and secondary systems can be represented as follows:

$$\begin{aligned} \theta_p(t) \quad &= \theta_p(t-1) + \tfrac{\tau}{mS} \Big[\textstyle\sum_z \gamma_z S_{cv}(z, t-1) \\ &\quad - \textstyle\sum_z \kappa_z S_{hv}(z, t-1) - \gamma_{ac} S_{ac}(z, t-1) \\ &\quad - \kappa_{ht} S_{ht}(z, t-1) \Big] \quad \forall t \in T \end{aligned} \tag{3.5}$$

The first term in the right hand side of (3.5) represents the inter-temporal dependency of inside temperature. The second and third terms model the effect of zonal valve openings on the main water loop temperature. The last two terms represents the effect of central AC and central heater operation on the main water loop temperature. When the temperature of water in the main water loop reaches the pre-defined upper temperature limit, the central AC is turned on to bring down the temperature of the water below this limit. A similar control mechanism takes place in the case of the central heater. The following constraints ensure successful implementation of these conditions:

$$S_{ac}(t) \geq \frac{\theta_p(t) - UB}{C_1} \tag{3.6a}$$

$$S_{ht}(t) \geq \frac{LB - \theta_p(t)}{C_1} \tag{3.6b}$$

Secondary System Modeling

In addition to the heat loss through walls, the secondary system model also includes: the heat loss through ventilation; activity level in different units; cooling and heating rate of zonal valve; cooling effect of fan operation; ambient room temperature; and the maximum temperature deviations that a resident is willing to tolerate. Since operational characteristics of cooling and heating systems are the same, these devices are modeled together, but only one of them operates at a time. Thus the room temperature is modeled as follows:

$$\begin{aligned}\theta_z(t) = \theta_z(t-1) + \frac{\tau}{C_z}\big[&\kappa_z S_{hv}(z,t) + \beta_{act} AL_z(t) \\ &- \gamma_z S_{cv}(z,t) + q_{f,z}(t) + \alpha_z(t)(\theta_{out} - \theta_{in})\big] \;\; \forall t \in T\end{aligned} \tag{3.7}$$

The first term in (3.7) represents the inter-temporal dependency of the room temperature. The second and fourth term represent the effect of zonal valve operation on inside temperature. The third term models the generated heat due to the activity level $AL_z(t)$ of the residents as proposed in [21]. Finally, the fifth term represents the effect of forced

air-circulation in the zone, and the last term represents the effect of heat loss through the outside wall of the unit.

The zonal supply fan equation is modeled as follows:

$$q_{f,z}(t) = \beta_z S_f(z,t)[S_m(z,t)\theta_{out}(t) - \theta_z(t)] \tag{3.8}$$

where the effect of air mixing and zonal fan's air circulation capability are included; it is assumed that the amount of fresh air entering the zone at any instant is equal to the amount of air exhausting from the respective zone. $S_{ac}(t), S_{ht}(t)$ and $S_f(z,t)$ are binary variables, i.e. 1 (ON) or 0 (OFF), while $S_{cv}(t), S_{hv}(t)$ and $S_m(z,t)$ are continuous variables ranging between 0 and 1.
The parameters $\alpha_z, \beta_z, \gamma_z, \kappa_z, \gamma_{ac}$ and κ_{ht} for the primary and secondary system models can be calculated by measurements or through a simple performance test using the following formulas:

$$\alpha_z = UA_z + \rho_a c_a Q_z^{leak} \tag{3.9a}$$
$$\beta_z = \rho_a c_a Q_z^{max} \tag{3.9b}$$
$$\gamma_{ac} = \eta_{ac} P_{ac}^{max} \times 3.6 \tag{3.9c}$$
$$\kappa_{ht} = \eta_{ht} P_{ht}^{max} \times 3.6; \tag{3.9d}$$
$$\gamma_z = \gamma_{ac} \frac{m_z}{m} \tag{3.9e}$$
$$\kappa_z = \kappa_{ac} \frac{m_z}{m} \tag{3.9f}$$

Operational Constraints

The central AC and the heater cannot be ON at the same time, which is ensured by the following constraint:

$$S_{ac}(t) + S_{ht}(t) \leq 1 \tag{3.10}$$

It is also to be noted that the operating states of the cooling $S_{cv}(t)$ and heating $S_{hv}(t)$ valves are dependent on the operational states of $S_{ac}(t)$ and $S_{ht}(t)$, respectively, as follows:

$$I_1(z,t) + I_2(z,t) \leq 1 \tag{3.11a}$$
$$S_{cv}(z,t) \geq C_2 I_1(z,t) \tag{3.11b}$$
$$S_{cv}(z,t) \leq I_1(z,t) \tag{3.11c}$$
$$S_{hv}(z,t) \geq C_2 I_2(z,t) \tag{3.11d}$$
$$S_{hv}(z,t) \leq I_2(z,t) \tag{3.11e}$$

The zonal supply fan is ON when the respective zonal valve (heating or cooling) is open. If the zonal supply fan is not ON, but the zonal valve is open, the cooling or heating coil can be damaged. Moreover, if any zonal supply fan is ON, the air mixer of that zone should also be ON, and vice-versa. These requirements are enforced using the following constraints:

$$S_f(z,t) = I_1(z,t) + I_2(z,t) \tag{3.12a}$$
$$C_2 S_f(z,t) \leq S_m(z,t) \leq S_f(z,t) \tag{3.12b}$$
$$FM(z,t) = C_2 S_f(z,t) - S_m(z,t) \tag{3.12c}$$
$$FM(z,t) \leq C_3 \tag{3.12d}$$

where (3.12b) ensures that, when any air mixing box is in operation at any instant, at least 10% of inside air is recirculated. Constraints (3.12c) and (3.12d) ensure that operational states of the zonal supply fan and air mixing unit are locked with each other.

In each zone, the zonal supply fan, the mixing box and the cooling/heating coil valves operate simultaneously but independently from those of other zones. However, if the outside temperature is less than θ_{out}^{min}, the zonal supply fan will stop circulating the outside air; this is enforced as follows:

$$S_f(z,t)(\theta_{out}(t) - \theta_{out}^{min}) \geq 0 \tag{3.13}$$

Finally, the inside temperature of each zone is bounded by upper and lower limits,

which are dynamic in nature and vary with time. These two limits are set by MURB residents to define their own comfort levels, and are represented as follows:

$$\theta_z^l(t) \leq \theta_z(t) \leq \theta_z^u(t) \tag{3.14}$$

3.2.3 Linearization of Constraints

The developed MURB model is a Mixed-Integer Non-Linear Programing (MINLP) problem. Hence, to reduce the computational burden of the model, some constraints are linearized by replacing the bi-linear terms; this linearization makes the model suitable for real-time application. Thus, consider S is a binary variable and $\aleph$ is a continuous variable which is bounded by one upper and lower limit as $\aleph^l \leq \aleph \leq \aleph^u$. The product $S.\aleph$ can be replaced by S_{com}, where S_{com} is defined by the following set of equations:

$$S_{com} \geq \aleph - (1 - S)\aleph \tag{3.15a}$$

$$S_{com} \leq \aleph \tag{3.15b}$$

$$S.\aleph^l \leq S_{com} \tag{3.15c}$$

$$S_{com} \leq S.\aleph^u \tag{3.15d}$$

These set of constraints are applied to the zonal supply fan (3.8) to replace the non-linear terms, yielding the following linear equation, which behaves exactly the same as the non-linear equation (3.8):

$$q_{f,z}(t) = \beta_z S_{com1}(z,t)\theta_{out}(t) - \beta S_{com2}(z,t) \tag{3.16}$$

where the product of $S_f(z,t)$ and S_m in (3.2) has been replaced by $S_{com1}(z,t)$, and the product of $S_f(z,t)$ and $\theta_z(t)$ has been replaced by $S_{com2}(z,t)$, with $S_{com1}(z,t)$ and $S_{com2}(z,t)$ satisfying (3.15).

3.3 Summary

In this chapter, the proposed hierarchical control architecture for the MURB CTCS is discussed. A comprehensive mathematical model for the optimal operation of the CTCS is presented, which includes the characteristics and operational constraints of all its components. A detailed description of inside temperature dynamics along with the calculation and discussion of the parameters are also presented. Finally, a linearization technique, which is adopted to reduce the computational complexity, is also discussed.

Chapter 4

Case Studies

4.1 MURB Example

Figure 4.1 shows the physical layout of a MURB used in this research, for testing and validation of the model presented in Chapter 3. An actual MURB from [22] is modified to set up realistic case studies. The MURB considered here has three floors, each floor has only one unit that is treated as a single zone, and each unit is 13m×10m×3m in size. Since no intra-zoning is considered within a unit, no intra-zonal heat flow takes place. The floor

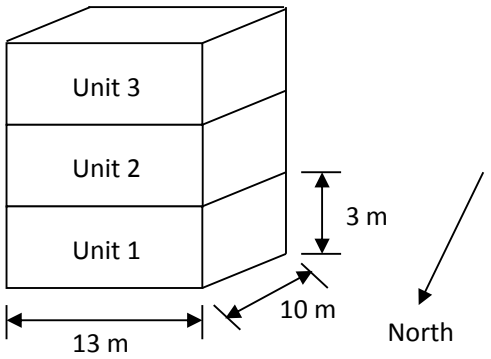

Figure 4.1: Geometric characteristics of an MURB.

heat flow is considered using the parameter α_z, denoting the heat loss through wall. All the walls, floors, and the roof are assumed to have the same physical properties.

The central cooling unit size is 124 kW, which provides necessary cooling for all the three units. Each zonal supply fan is rated at 0.7457 kW. The air mixing unit consumes very little energy when closing and opening the valves; hence, its energy consumption is neglected. The heat exchange between the primary and the secondary system is considered to be ideal.

4.2 Model Inputs

The following are the inputs used in this work:

- Two different electricity prices are used here: Time of Use (TOU) and Real Time Pricing (RTP) for Ontario. TOU is the simplest form of dynamic pricing scheme, in which there are three price periods: peak, mid-peak and off-peak; these periods vary with season and day of the week. As in Chapter 2, the RTP is assumed to be the HOEP, as posted by the IESO, neglecting price adjustments applied to obtain the actual consumer price [36]. An example of these two pricing scheme is given in Fig. 4.2.

- A fixed pricing scheme is considered for natural gas pricing, although the price may vary according to the suppling company and zones in Ontario. The average price of household supply gas, considered in this work, is 0.130806 $\$/m^3$ [37].

- Fifteen minute intervals are considered as time steps for the model simulations to determine the optimal set-points of the decision variables.

- Temperature limits are set by the units' residents as per their own preferences for comfort and energy savings. In this work, the limits are chosen based on [38]. The lower and upper limits for each MURB unit are shown in Table 4.1.

Table 4.1: Temperature limits for MURB units

Unit	Levels	12AM-9AM	9AM-6PM	6PM-12AM
1	Lower	20	20	20
	Upper	22	24	22
2	Lower	20	20	20
	Upper	23	25	23
3	Lower	20	20	20
	Upper	24	26	24

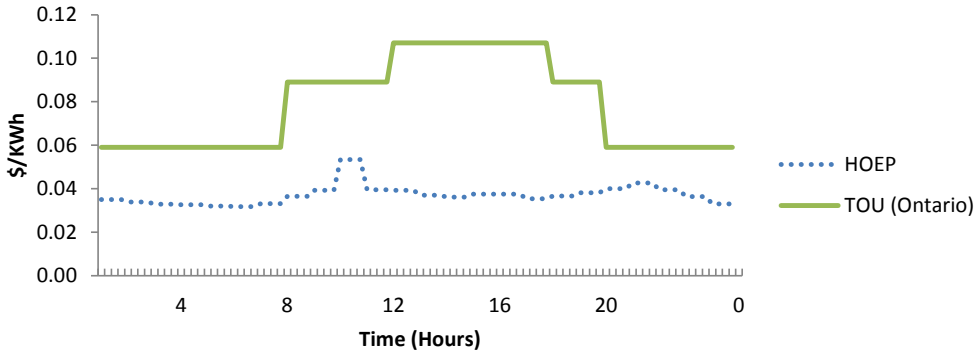

Figure 4.2: Electricity pricing schemes of a summer weekday in Toronto (Jul 22, 2011) [31].

- The effect of customers' activity and occupancy of the unit is modeled through the Activity Level parameter proposed in [21]. The estimation of this parameter is typically based on historical energy consumption data. Figure 4.3 shows the chosen activity level for all units used in this work.

- Outside temperature data for the Toronto region is used here [32]. Figure 4.4 shows the outside temperature variation of a warm summer day in Toronto (Jul 22, 2011).

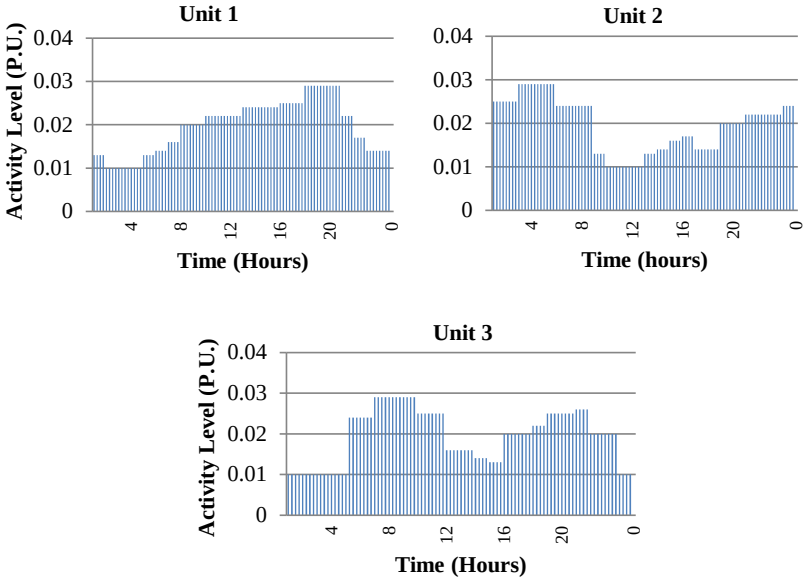

Figure 4.3: Activity level for all units.

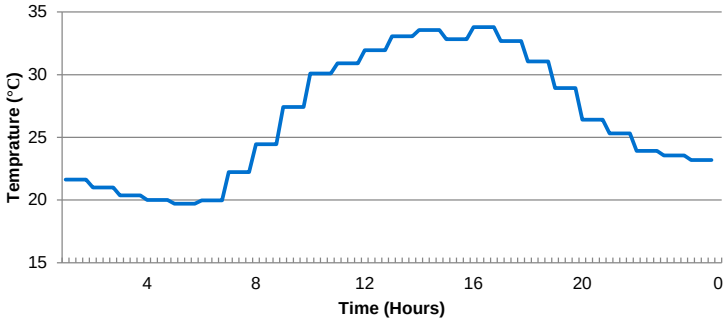

Figure 4.4: Temperature of a warm summer day in Toronto (Jul 22, 2011).

4.3 Results and Analysis

The following are the case studies analyzed in this work:

- Case 0: In this case, the proposed MURB optimization model seeks to maximize the comfort levels of the residents by minimizing the temperature deviation from their respective set points. This case is considered as a realistic base case, since it reflects

the operation of the existing temperature control systems, and thus establishes a reference for comparison purposes.

- Case 1: In this case, the objective is to minimize the energy consumption cost of the CTCS, assuming that residents in different units have the same "rational" objective of minimizing their energy cost. This scenario reflects a typical MURB owner's point of view.

- Case 2: In this case, the objective is to minimize the energy consumption of the CTCS only. Thus, the objective function is independent of the pricing schemes and reflects a typical Load Distribution Companies' (LDCs) point of view.

4.3.1 TOU Pricing

Figures 4.5a, 4.5b and 4.5c present the variation of indoor temperature of Zone 1 for Case 0, 1, and 2, respectively, for the TOU pricing scheme. Since the customers' comfort level is maximized in Case 0, the operation schedule of the cooling valve is not optimized, i.e. the number of operations of the cooling valve is high, thus increasing the main water loop temperature rapidly, which leads to a higher number of operations of the central AC. On the other hand, as shown in Figures.4.6b and 4.6c, in Case 1 and 2, where energy cost and energy consumption are minimized, respectively, by the optimal operation of the cooling coil valve while satisfying other constraints; the number of operation of the central AC is lower. Note that the optimization model turns ON the central AC during the low price period only when it is necessary. Optimal operation schedules of the cooling valve, supply fan and air mixing unit for the respective zones are also shown in these figures.

Figure 4.6 presents the optimal operation schedules of the central AC for Case 0, 1 and 2. All these optimized schedules are obtained using the proposed supervisory CTCS for the MURB.

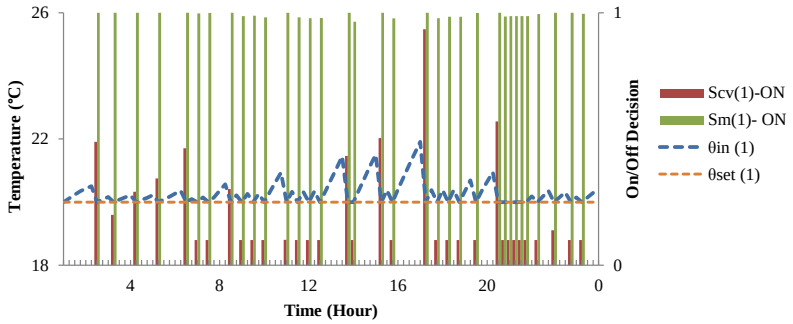

(a) Case 0

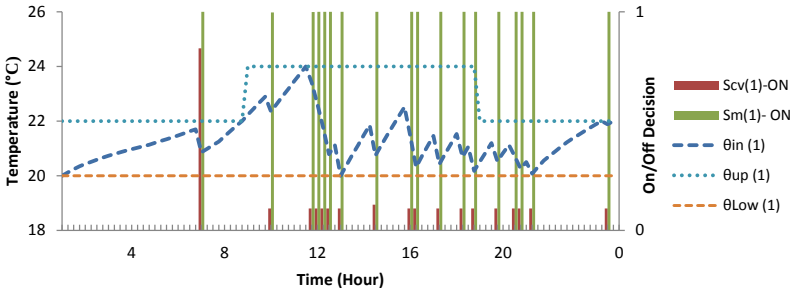

(b) Case 1

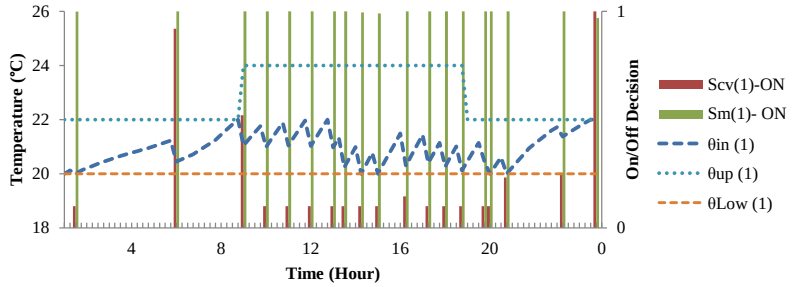

(c) Case 2

Figure 4.5: Indoor temperature variation of Zone 1 for different Cases, with TOU.

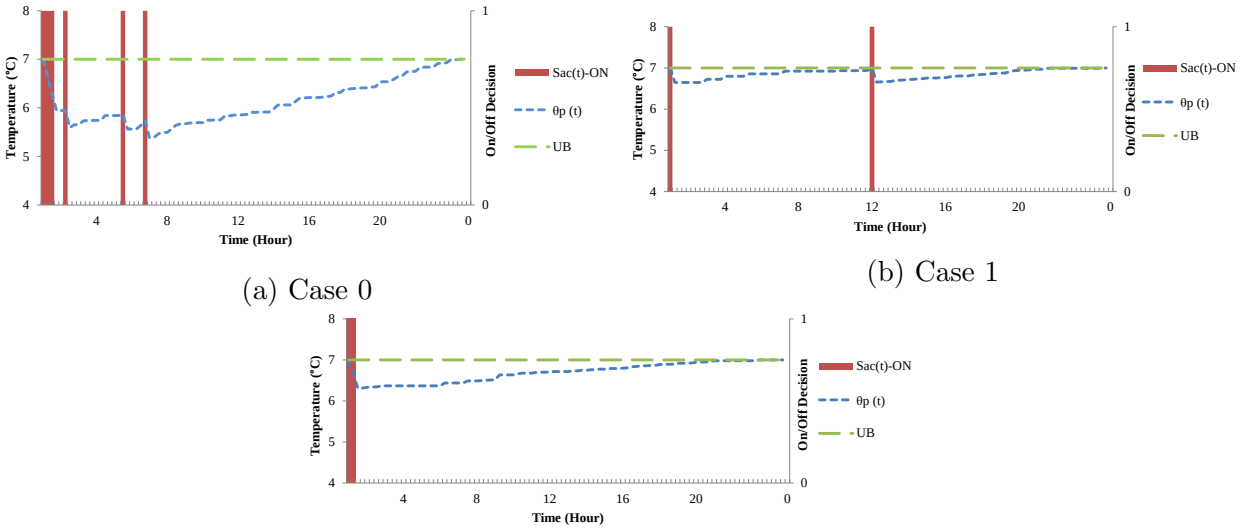

(a) Case 0

(b) Case 1

(c) Case 2

Figure 4.6: Optimal schedule of central AC for different Cases, with TOU.

4.3.2 RTP Scheme

Figures 4.7a, 4.7b, and 4.7c present the variation of indoor temperature of Zone 1 for Case 0, 1, and 2, respectively, considering the assumed RTP scheme. The pattern of variation of indoor temperatures are almost the same as those with TOU pricing, since, all other constraints are the same for the both cases. These variations are caused due to the different timings of low price periods in these two pricing schemes. The frequent valve operations lead to the larger number of central AC operations in this case.

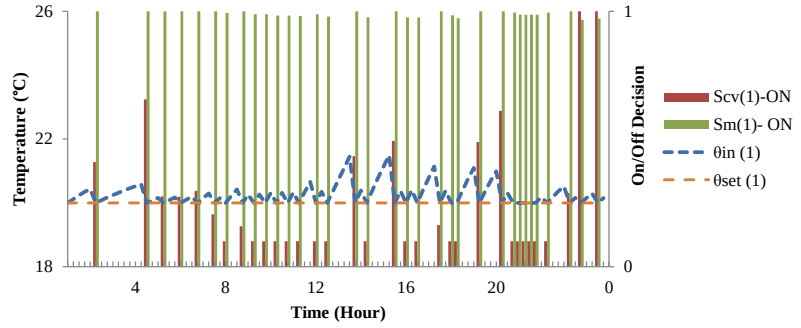

(a) Case 0

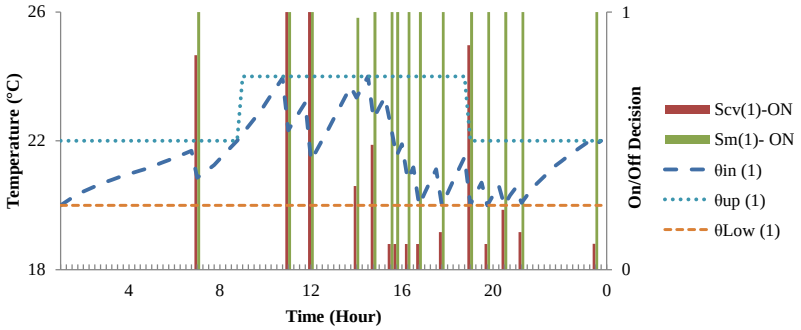

(b) Case 1

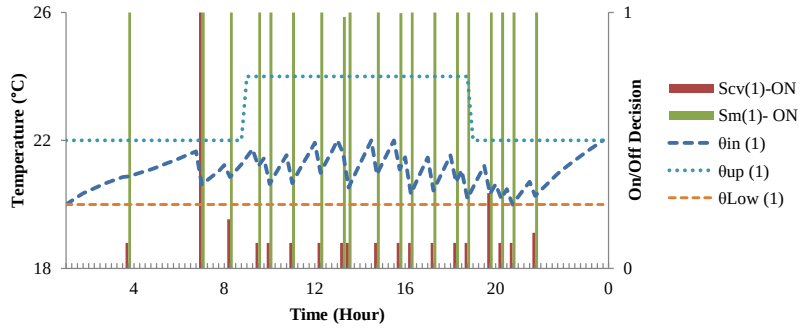

(c) Case 2

Figure 4.7: Indoor temperature variation of Zone 1 for different cases, with HOEP.

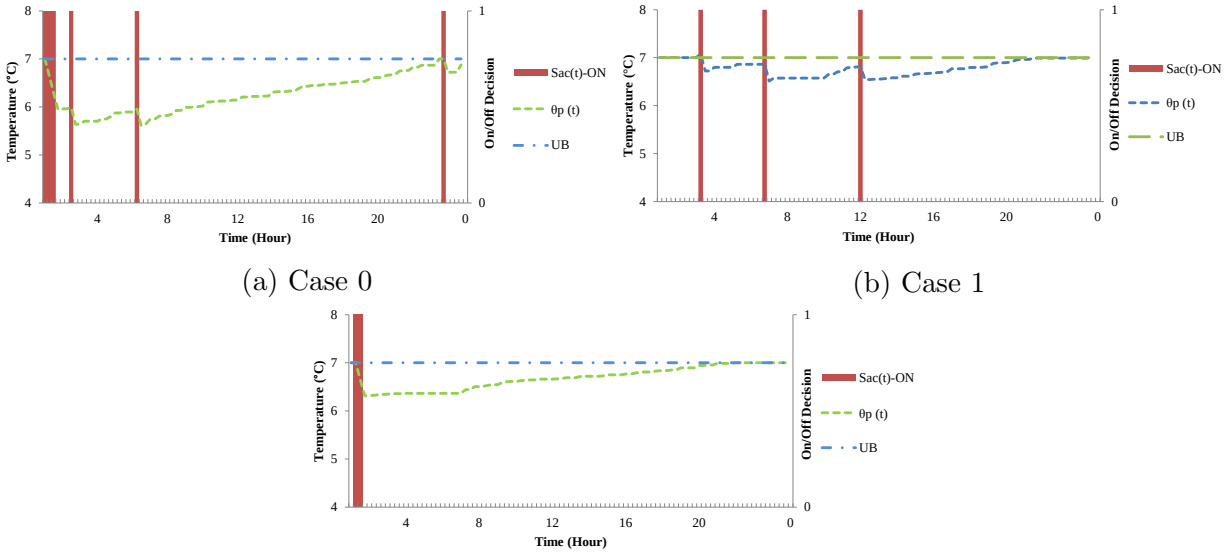

(a) Case 0

(b) Case 1

(c) Case 2

Figure 4.8: Optimal schedule of central AC for different cases, with HOEP.

Table 4.2: Comparison of electrical energy consumption and cost

Cases	HOEP		TOU	
	Cost ($)	Energy (kWh)	Cost ($)	Energy (kWh)
Case 0	19.308	572.541	35.766	572.168
Case 1	10.871	287.762	16.724	195.694
Case 2	6.696	196.999	12.529	196.999

Table 4.2 presents a comparison of the total electrical energy consumption and cost for the three case studies and the two different pricing schemes. Observe that, for HOEP and TOU, Case 2 results in the lowest cost as compared to the other cases, while the maximum total cost is obtained for Case 0. The objective function of Case 1 is cost minimization, and of Case 2 is energy consumption minimization, but the lowest cost is obtained for Case 2; this occurs because of the presence of multiple local optimal solutions of the non-linear optimization problem.

Table 4.3 presents a comparison of savings in energy consumption and cost with respect

Table 4.3: Comparison of savings in total energy consumption and cost

Cases	HOEP Savings %		TOU Savings %	
	Cost	Energy	Cost	Energy
Case 0	-	-	-	-
Case 1	43.696	49.739	53.24	65.8
Case 2	65.32	65.57	64.97	65.57

to the base case (Case 0). Compared to the base case, over 40% savings in electricity cost and energy consumption can be observed in both Case 1 and Case 2.

4.3.3 Multi-Objective Optimization

In this section, a case study is formulated wherein the residents in different units of the MURB have different preferences and priorities. For example, the resident in Unit 1 may seek to maximize the comfort level, while the resident in Unit 2 seeks to minimize energy cost. In such a case, finding a Pareto optimal solution, considering each customer's preferences is not possible, because the individual objective functions present the same behavior, i.e. energy costs decrease as energy consumption decreases. Therefore, appropriate weighting factors are chosen instead in (3.4) to weigh the customers' different objective functions that best match their interests. For this study, the MURB model is reduced from three to two units (i.e. σ=0), and all parameters are suitably scaled, varying the respective weighting factors μ and ψ from 0 to 1, with a 0.1 step size. Several combinations of μ and ψ give the same total energy cost, but the value of J_M can be different, as illustrated in Figures. 4.9 and 4.10. The minimum cost obtained is 6.566 \$/day for μ =0.3 and ψ=0.8, and the highest cost of 15.678 \$/day is obtained for μ =0.8 and ψ=1.0. However, it is evident from the results that a high value of μ for Unit 1's objective function results in comparatively higher cost for Unit 2, despite having a lower weighting factor for its objective function. Moreover, equal importance attached to the two objective functions (μ =0.5 and ψ=0.5) results in higher costs (11.912 \$/day) as compared to the obtained least cost (6.566 \$/day).

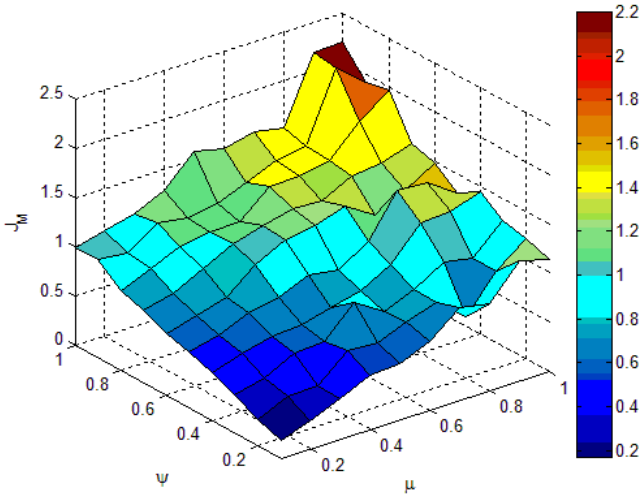

Figure 4.9: Variation of J_M with the variation of multi-objective function weights.

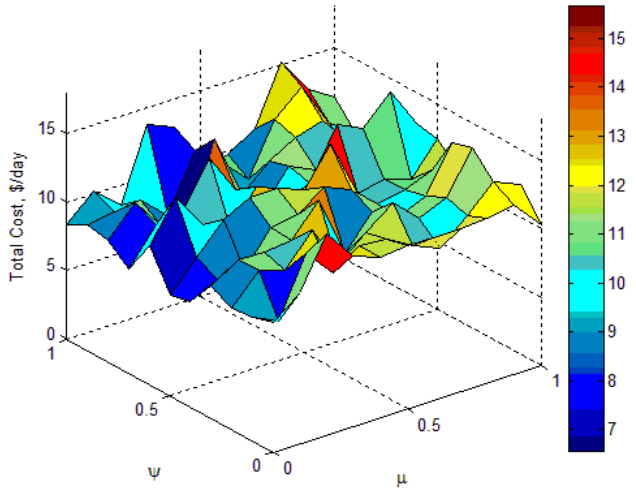

Figure 4.10: Variation of total cost with the variation of multi-objective function weights.

While optimizing the composite objective function J_M with the variation of weights μ and ψ for J_1 and J_2, respectively, the changing patterns of these two functions exhibit similar characteristics as the total cost function rather than the composite objective function J_M, as shown in Figures. 4.11a and 4.11b. The Unit 1's residents preference is to maintain their own temperature setting fixed, while the Unit 2's residents preference is to minimize

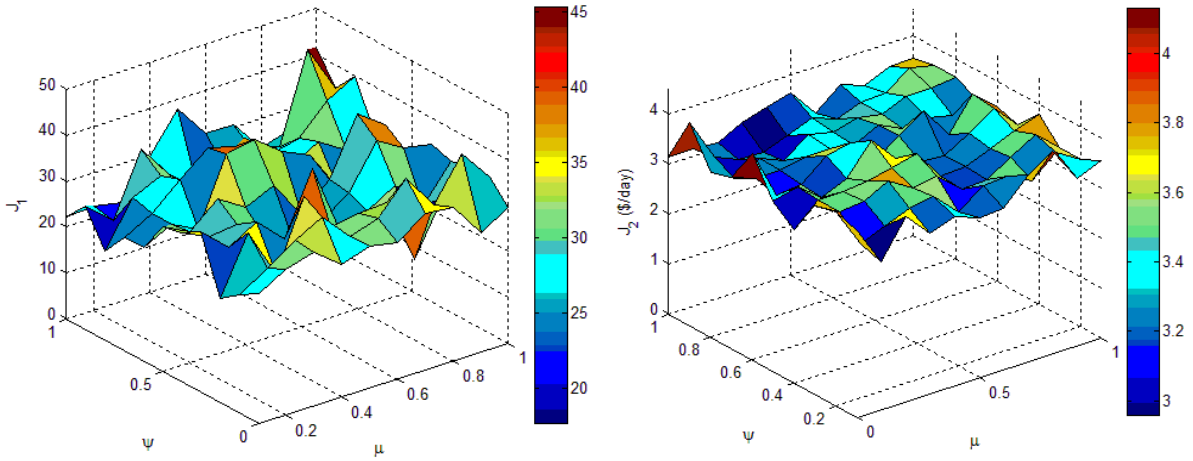

(a) J_1 (b) J_2

Figure 4.11: Variation of J_1 and J_2 with the variation of multi-objective function weights.

energy cost. The higher values of μ and ψ result in the lower temperature deviation in Unit 1 and energy cost in Unit 2, respectively. When μ= 1, the value of J_1 is minimum, and the value of J_2 is comparatively higher in spite of the lower value of ψ. Thus, in a CTCS system, one customer's preference affects the other customer's preference as well. This phenomenon occurs because the energy consumption cost of CTCS should be divided among all customers proportionately to their consumption after each interval, which is also a common practice for CTCS for an actual MURB. However, the total energy consumption of the CTCS also exhibits the same characteristics of total cost function; since the energy consumption of the CTCS decreases or increases, the total cost also decreases or increases simultaneously, as illustrated in Figure 4.12.

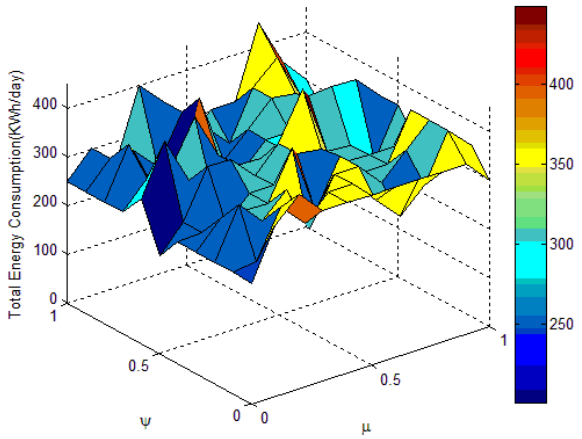

Figure 4.12: Variation of total energy consumption with the variation of multi-objective function weights.

4.4 Computational Aspects

The proposed CTCS model of the MURB is a Mixed Integer Non-Linear Programing (MINLP) problem, implemented in GAMS using the Simple Branch and Bound (SBB) solver, which is based on the NLP MINOS solver [39]. The computational statistics of the proposed model are as follows:

- Number of zones: 3
- Number of time intervals: 96 (1 day, 15 min each)
- Number of continuous variables: 4633
- Number of binary variables: 1248
- Number of equations (including system and constraints): 7893
- Execution time : $\sim$ 30-60s

The constraint linearization, as discussed in Chapter 3, reduces the computational burden such that the optimal solutions can be obtained in less than 1 minute, on average, which makes the proposed control approach suitable for the real-time applications.

4.5 Summary

This chapter presented the results of different case studies, for the MURB CTCS model presented in Chapter 3, to determine the model's effectiveness and performance. The obtained simulation results showed that significant cost savings, in the order of 40%, would be obtained when minimization of energy cost or energy consumption are considered as objectives for the proposed supervisory control system. Finally, the model's capability and efficiency was verified through a multi-objective optimization study, wherein different units of the MURB had conflicting preferences.

Chapter 5

Conclusions and Future Work

5.1 Summary and Conclusions

This thesis explored the application of EMS for the real-time integration of MURB energy hub into smart grids under a DR paradigm. A comprehensive mathematical model was proposed in this work for the smart operation of CTCS of a MURB. The inside temperature dynamics of the MURB was modeled considering its complex thermodynamical properties, and all the parameters were suitably scaled for an approximate representation of the building's physical characteristics. The temperature control devices of CTCS, i.e., central heating and cooling unit, zonal fan unit, air mixing unit, and cooling or heating valves in each zones, were included into the model to maintain the inside temperature within customers' predefined ranges. The proposed model sought the real-time operation schedules of the CTCS while optimizing different customers' desired objectives. The developed model incorporated weather forecast, electricity price information, and the end-users' preference settings as inputs to the supervisory control system. It was observed that the proposed control strategy may yield over 40% savings in electrical energy costs. The impact of conflicting users' objectives in a MURB were also studied based on a multi-objective optimization approach, demonstrating that in this case, there is no Pareto-optimal solution.

5.2 Contributions

The main contributions of this work can be summarized as follows:

- A comprehensive mathematical model for real-time temperature control of a MURB has been developed to generate optimal set points for temperature control devices of the CTCS, considering central heating/cooling unit, zonal supply fan, and air mixing units.
- A supervisory control strategy of CTCS based on the proposed mathematical model of MURBs has been proposed, demonstrating with realistic studies that significant energy and cost savings can be obtained.

5.3 Future Work

The scope for future work pertaining to the CTCS of a MURB can be as follows:

- In this work, each unit of the MURB is considered as a single zone, i.e. there is no intra-zoning in a unit. However, a more comprehensive and detailed zonal model could be developed dividing each zone into several sub-zones, requiring the development of an intra-zonal heat flow model.
- A humidifier and dehumidifier model in the cooling/heating coil could also be incorporated for maintaining proper humidity levels inside the MURB.
- The proposed supervisory control strategy could be tested in an actual MURB for validation purposes.

Bibliography

[1] Canadian Energy Overviews 2011- Energy Briefing, National Energy Board. [Online]. Available: http://www.neb-one.gc.ca/clf-nsi/rnrgynfmtn/nrgyrprt/nrgytlk/nrgytlk-eng.html

[2] Canada's energy future: Energy supply and demand projections to 2035. [Online]. Available: http://www.neb-one.gc.ca/clf-nsi/rnrgynfmtn/nrgyrprt/nrgyftr/nrgyftr-eng.html

[3] "Ontario's Long-Term Energy Plan". [Online]. Available: http://www.energy.gov.on.ca/docs/en/MEI_LTEP_en.pdf

[4] "2011 Annual Report- Reliable Power For Ontario's Future". [Online]. Available: http://www.ieso.ca/imoweb/pubs/corp/IESO_2011AnnualReport.pdf

[5] T. Martin. "Life in metropolitan areas". [Online]. Available: http://www.statcan.gc.ca/pub/11-008-x/2008001/article/10459-eng.htm

[6] R. Liu. (2007) Energy Consumption and Energy Intensity in Multi-Unit Residential Buildings in Canada. [Online]. Available: http://www.cbeedac.com/publications/documents/MURBsrp04.pdf

[7] (2010, April) Households and the environment: Energy use. [Online]. Available: http://www5.statcan.gc.ca/bsolc/olc-cel/olc-cel?catno=11-526-SWE&lang=eng

[8] U.S. Department of Energy, "Your Home's Energy Use", Aug. 2012. [Online]. Available: http://energy.gov/energysaver/articles/tips-your-homes-energy-use

[9] (2010, September) The smart grid: An introduction. [Online]. Available: http://energy.gov/sites/prod/files/oeprod/DocumentsandMedia/DOE_SG_Book_Single_Pages(1).pdf

[10] K. Moslehi and R. Kumar, "A reliability perspective of the smart grid," *IEEE Trans. Smart Grid*, vol. 1, no. 1, pp. 57 –64, june 2010.

[11] A. Bose, "Smart transmission grid applications and their supporting infrastructure," *IEEE Trans. Smart Grid*, vol. 1, no. 1, pp. 11 –19, june 2010.

[12] M. Behrangrad, H. Sugihara, and T. Funaki, "Analyzing the system effects of optimal demand response utilization for reserve procurement and peak clipping," in *Power and Energy Society General Meeting, 2010 IEEE*, 2010, pp. 1–7.

[13] Federal Energy Regulatory Commission, "Assessment of demand response and advanced metering", Feb 2010. [Online]. Available: http://www.ferc.gov/legal/staff-reports/2010-dr-report.pdf

[14] V. Balijepalli, V. Pradhan, S. Khaparde, and R. M. Shereef, "Review of demand response under smart grid paradigm," in *Innovative Smart Grid Technologies - India (ISGT India), 2011 IEEE PES*, 2011, pp. 236–243.

[15] Ontario Power Authority, "Demand Response Program",. [Online]. Available: http://www.powerauthority.on.ca/category/keywords/demand-response

[16] S. Ahmad, "Smart metering and home automation solutions for the next decade," in *Emerging Trends in Networks and Computer Communications (ETNCC), 2011 International Conference on*, 2011, pp. 200–204.

[17] G. Koutitas, "Control of flexible smart devices in the smart grid," *IEEE Trans. Smart Grid*, vol. 3, no. 3, pp. 1333–1343, 2012.

[18] F. Rahimi and A. Ipakchi, "Demand response as a market resource under the smart grid paradigm," *IEEE Trans. Smart Grid*, vol. 1, no. 1, pp. 82–88, 2010.

[19] V. Silva, V. Stanojevic, D. Pudjianto, and G. Strbac. (2011, Sept.) Value of Smart Domestic Appliances in Stressed Electricity Networks: Smart-A. Imperial College, University of Manchester, London UK. [Online]. Available: http://www.smart-a.org/W_P_4_D_4_4_Energy_Networks_Report_final.pdf

[20] (2003) Blueprint for Demand Response in Ontario. [Online]. Available: http://sites.energetics.com/MADRI/toolbox/pdfs/ontario/blueprint.pdf

[21] M. C. Bozchalui, S. Hashmi, H. Hassen, C. Cañizares, and K. Bhattacharya, "Optimal operation of climate control systems of produce storage facilities in smart grids," *IEEE Trans. on Smart Grid*, vol. 3, no. 4, Dec. 2012.

[22] R. Barbosa and N. Mendes, "Combined simulation of central HVAC systems with a whole-building hygrothermal model," *Energy and Buildings*, vol. 40, no. 3, pp. 276–288, 2008.

[23] C. Marnay, G. Venkataramanan, M. Stadler, A. Siddiqui, R. Firestone, and B. Chandran, "Optimal technology selection and operation of commercial-building microgrids," *IEEE Transactions on Power Systems*, vol. 23, no. 3, pp. 975–982, 2008.

[24] A. Elmoudi, O. Asad, M. Erol-Kantarci, and H. T. Mouftah, "Energy consumption control of an air conditioner using web services," *IEEE Smart Grid and Renewable Energy*, vol. 2, no. 3, pp. 255–260, 2011.

[25] R. Hämäläinen and J. Mäntysaari, "Dynamic multi-objective heating optimization," *European Journal of Operational Research*, vol. 142, no. 1, pp. 1–15, 2002.

[26] K. Schneider, J. Fuller, and D. Chassin, "Analysis of distribution level residential demand response," in *Power Systems Conference and Exposition (PSCE), 2011 IEEE/PES*, 2011, pp. 1–6.

[27] C. Roe, S. Meliopoulos, R. Entriken, and S. Chhaya, "Simulated demand response of a residential energy management system," in *Energytech, 2011 IEEE*, 2011, pp. 1–6.

[28] M. Kim, I. Yook, D. Kim, L. Kim, and J. Kim, "Study on simulation modelling strategy for predicting thermal energy demand profiles of residential complex," in *11th Int. IBPSA Building Simulation Conf. 09*, Glasgow, Scotland, July 2009.

[29] R. Yang and L. Wang, "Multi-objective optimization for decision-making of energy and comfort management in building automation and control," *Sustainable Cities and Society*, 2011.

[30] M. Rahman and S. Yamashiro, "Novel distributed power generating system of pv-ecass using solar energy estimation," *IEEE Trans. on Energy Conversion*, vol. 22, no. 2, pp. 358–367, 2007.

[31] IESO Public Reports, Market data, July. 2011. [Online]. Available: http://ieso.ca.htm.

[32] National Climate Data and Information Archive. [Online]. Available: http://climate.weatheroffice.gc.ca/climateData/canada_e.html

[33] University of Toronto, Department of Geography, Weather data, July, 2011. [Online]. Available: http://www.utm.utoronto.ca/geography/resources/meteorological-station/weather-data

[34] A. Bhatia. Centralized versus decentralized air conditioning systems. [Online]. Available: http://www.seedengr.com/Cent%20Vs%20Decent%20AC%20Systems.pdf

[35] ASHRAE Handbook-HVAC Applications, 2011. [Online]. Available: http://www.ashrae.org

[36] Canadian Electricity Association, "Overview of Electricity Regulation in Canada, 2008."

[37] Ontario Eenergy Board. [Online]. Available: http://www.ontarioenergyboard.ca

[38] H. Burroughs and S. J. Hansen, *Managing Indoor Air Quality*, 5th ed. Fairmont Pr, 2011, vol. 1.

[39] *GAMS-The Solver Manuals*, GAMS Development Corporation, Washington-USA, Dec 2012.